UCRL-18154

cy. 2

University of California
Ernest O. Lawrence Radiation Laboratory

TWO-WEEK LOAN COPY

This is a Library Circulating Copy which may be borrowed for two weeks. For a personal retention copy, call Tech. Info. Division, Ext. 5545

N* STUDIES VIA πp INELASTIC REACTIONS

Arthur H. Rosenfeld and Paul H. Söding

March 29, 1968

Berkeley, California

UCRL-18154

DISCLAIMER

This document was prepared as an account of work sponsored by the United States Government. While this document is believed to contain correct information, neither the United States Government nor any agency thereof, nor the Regents of the University of California, nor any of their employees, makes any warranty, express or implied, or assumes any legal responsibility for the accuracy, completeness, or usefulness of any information, apparatus, product, or process disclosed, or represents that its use would not infringe privately owned rights. Reference herein to any specific commercial product, process, or service by its trade name, trademark, manufacturer, or otherwise, does not necessarily constitute or imply its endorsement, recommendation, or favoring by the United States Government or any agency thereof, or the Regents of the University of California. The views and opinions of authors expressed herein do not necessarily state or reflect those of the United States Government or any agency thereof or the Regents of the University of California.

For Proceedings of the
Conference on πN Interactions,
Dec. 1-2, 1967, Irvine, California

UCRL-18154
Preprint

UNIVERSITY OF CALIFORNIA

Lawrence Radiation Laboratory
Berkeley, California

AEC Contract No. W-7405-eng-48

N^* STUDIES VIA πp INELASTIC REACTIONS

Arthur H. Rosenfeld and Paul H. Söding

March 29, 1968

For Proceedings of the
Conference on πN Interactions,
Dec. 1-2, 1967, Irvine, California

UCRL-18154

N^* STUDIES VIA πp INELASTIC REACTIONS

Arthur H. Rosenfeld and Paul H. Söding*

Department of Physics and Lawrence Radiation Laboratory
University of California
Berkeley, California

March 29, 1968

INTRODUCTION

Most of our knowledge of non-strange baryonic resonances has come from "elastic (scattering) phase shift analysis" (EPSA)

$$\pi p \text{ (partial waves)} \rightarrow \pi p, \tag{1}$$

as discussed at this conference by Lovelace and Steiner.

In this paper we give:

I. A brief survey of inelastic cross sections (mainly via figures) and experiments (via two tables).

II. A summary of what very little extra insight (beyond that from EPSA) has come so far from the inelastic final states of N^* resonances when these are formed in the s channel

$$\pi p \rightarrow N^* \rightarrow \pi\pi N, \eta N, K\Lambda, \cdots . \tag{2}$$

III. A discussion of what useful information (branching ratios and signs of amplitudes) may be expected in the next year or so, and their relation to SU(3) classification.

We considered, but did not write, a Section IV on the production of N^*'s in reactions like $\pi p \rightarrow \pi N^*$, $pp \rightarrow N^* p$. However, we concluded that these experiments, while valuable as studies of the production process, are not yet very illuminating in our context. They do yield

significant bumps[1] at N^*(1400, 1512, 1688, $\cdots$), and Δ(1236 and 1920), and also a bump in the $\pi^+\pi^+p$ spectrum at 1560 MeV.[2] However, the N^* (1400) bump seems to involve constructive interference of both the P_{11} resonance production and diffraction dissociation,[3] the N^*(1512 and 1688) bumps probably involve several unresolved resonances, and the $\pi^+\pi^+p$ (1560) could well be a kinematic effect.[2]

I. BRIEF PICTORIAL SURVEY

First we summarize π^-p cross-section information[4,5] in Fig. 1. The difference between σ_{tot} and the sum of the lower curves is of course essentially made up by charge exchange. For $N^*_{3/2}$ resonances, $\sigma_{c.e.}/\sigma_{el} = 2/1$; for $N^*_{1/2}$, $= 1/2$. As we shall see in Fig. 4, the most abundant $\pi\pi N$ channel is $\pi^+\pi^-n$, then comes $\pi^-\pi^0p$, then $\pi^0\pi^0n$.

The Fig. 1 insert is a compact way of indicating the energy dependence of the population of the Δ(1236) bands of the $\pi^+\pi^-n$ Dalitz plot. The bars, solid and open, are experimental ratios; the curve, for comparison, shows where the <u>sum</u> of the two Δ bands would fall if the Dalitz plot population were uniform.

A typical $\pi^+\pi^-n$ Dalitz plot at $T_\pi = 900$ MeV ($\sqrt{s} = 1688$ MeV) is shown in Fig. 2. Half the dots fall in the Δ^-(1238) band, even though it occupies only 15-20% of the area. The Δ^+ band shows no enhancement ($n\pi^+$ is much less strongly coupled to $I = 3/2$). These facts are noted in the insert to Fig. 1 as a solid bar at 50% population for $T_\pi = 900$ MeV, an open bar at 25%, and a solid line at about 36% which represents the sum of the fractional areas of the two bands. The insert shows that $\pi^+\Delta^-$ is the dominant final state in $\pi^-p \rightarrow \pi\pi N$ over a large energy range. This should simplify the partial-wave analysis.

Figure 3 surveys π^+p cross sections.[6] Most of the comments that we made for π^- in Fig. 1 also apply to Fig. 3. Here there are only two charge states, $\pi^+\pi^0p$ and $\pi^+\pi^+n$.

Figure 4 apportions the total $\sigma(\pi\pi N)$ of Fig. 1 (π^-p) and Fig. 3 (π^+p) into the individual charge channels,[7] and gives some measure of the consistency of the experimental data. Note the dominance of the two channels ($\pi^+\pi^-n$ and $\pi^+\pi^0p$) where we expect, and find, large Δ-band enhancements. To expand on this point we write down here Eqs. (3^-) and (3^+), which are just a display of some products of squares of Clebsch-Gordan coefficients. We assume that the three $(\pi\pi N)^0$ channels come from a pure $I = 1/2$ amplitude $\pi^-p \to N^{*0}_{1/2} \to \pi\Delta$. Then the resulting relative populations of the Δ bands are:

$$\underbrace{\pi^+n\pi^-}_{1+9=10} : \underbrace{\pi^0p\pi^-}_{2+2=4} : \underbrace{\pi^0n\pi^0}_{4}. \qquad (3^-)$$

Similarly for $\pi^+p \to N^{*++}_{3/2} \to \pi\Delta$, we have

$$\underbrace{\pi^+p\pi^0}_{9+4=13} : \underbrace{\pi^+n\pi^+}_{2}. \qquad (3^+)$$

The experimental cross sections of Fig. 4 are in fact ordered in size in just the sequence given by Eqs. (3).

So far our pictorial survey has been too crude to mention partial waves; however, from EPSA one can of course predict the size of the inelastic partial waves; in fact Eqs. (4) show that σ_{inel} is just proportional to the hatched area on the Argand plot of Fig. 5. To see this, just compare[8]

$$\sigma_{el} = 4\pi\lambda^2 (J + \tfrac{1}{2}) \, |T|^2 = 4\pi\lambda^2 (J + \tfrac{1}{2}) \left| \frac{\eta \exp(2i\delta) - 1}{2i} \right|^2 , \quad (4\ el)$$

$$\sigma_{inel} = \pi\lambda^2 (J + \tfrac{1}{2})(1 - \eta^2) = 4\pi\lambda^2 (J + \tfrac{1}{2})[(\tfrac{1}{2})^2 - (\tfrac{\eta}{2})^2]. \quad (4\ inel)$$

Next we turn to the available experimental data, which we list in two tables:

Table I ($\pi^- p \to \pi\pi N$). Two dozen small hydrogen bubble chamber experiments have been published with anywhere from a few hundred to 2000 inelastic events each, or a total of 23 000 events in all. Experiments now underway are listed in parentheses. A European effort is now aiming at 40 000 inelastic events per year, and an LRL-SLAC collaboration is comparable. (LRL-SLAC exposures are indicated as inserts of ~2000 inelastic events each.)

Table II ($\pi^+ p \to \pi\pi N$). The published data are comparable with those of Table I, but there does not seem to be as much interest in large new runs, presumably because in this energy range there seem to be fewer Δ resonances to be sorted out, than $N^*_{1/2}$ resonances.

II. INELASTIC PARTIAL-WAVE ANALYSES

To physicists familiar with the great successes of hydrogen bubble chamber s-channel resonance formation experiments in discovering and identifying $Y^*_0(1520)$, $Y^*_1(1660)$, $Y^*_1(1770)$, and many others, it can be surprising that similar experiments with $\pi p \to \pi\pi N$ have yielded much less information.

The explanation is probably that until recently $K^- p$ experiments seemed more promising than those with πp, for several reasons:

a) the Y^* resonances seemed to be narrower, hence easier to resolve,

and more numerous;

b) copious inelastic final states like $\pi\Lambda$, $\pi\Sigma$, $\pi\Lambda(1520)$, are two-body, or quasi-two-body, and hence easier to analyze than $\pi\pi N$;

c) the subsequent K or Y decays make it possible to observe even neutral particles, and yield extra data on the weak interaction, making each event more informative.

Anyway, whatever the reasons, the largest bubble chamber groups tended to build electrostatically separated K^- beams, collect and measure hundreds of thousands of events, and carry out detailed partial-wave fits to the data.

By contrast, πp experiments were considered less exciting and have really only become reputable with the advent of high-quality polarization data and the thorough phase shift analyses. In fact this conference is an example of reawakened interest. Until recently, the πp inelastic channels tended to be studied by smaller, more dispersed groups, who measured fewer events and got less from each measurement.

Just as the πp data are less complete than the K^-p data, so correspondingly less effort has gone into understanding them.

At a given c.m. energy in a three-body final state (e.g., $\pi\pi N$, or $\pi\Delta$, where $\Delta \rightarrow \pi N$) the momenta are specified by four independent variables, which can be thought of as the two coordinates "internal" to the Dalitz plot, and two "external" angles, specifying for example the c.m. production angle θ_1 of particle 1, and the azimuth angle ϕ_{23} between the planes of production and decay of the diparticle (23). The Kp style of operating has been to write onto a data summary tape these

four variables for each event, then make a partial-wave fit to all these data. Sometimes data from several experiments have then been pooled to extend the energy range and improve the statistics.

The πp analyses have been much less powerful. The early advocates of an "isobar model" were Sternheimer and Lindenbaum,[9] and later Olsson and Yodh.[10] Both papers fitted only mass and angular distributions. Let us discuss what fraction of the information one loses thereby. Since we are dealing with partial waves up to $J = 7/2$, we expect Legendre polynomials up to $P_7(\cos\theta)$ to show up in an expansion. Hence a proper treatment would assign 10 to 20 bins to each variable; then in the space of all four variables we expect more than 10^4 significant bins. Instead the current style is to fit at most the three (correlated) projections of the Dalitz plot and (omitting the correlations) about three more production angles, one for each particle. To our disappointment, it is hard to say how much information is thus lost, but it seems to be considerable.

We know of nobody so far who has bothered to collect any appreciable fraction of the total data available and make a complete fit. As we said above, now that the EPSA's have shown us there are many resonances under each bump, waiting for their $\pi\pi N$ modes to be disentangled, the field has become reputable, and you may expect things to change. But it will take a year. Meanwhile, and with apologies, let us discuss what little has been learned so far.

1. <u>$I = 1/2$, $\pi N \to \pi\pi N$</u>

From the phase shift analyses of elastic pion-nucleon scattering, it is known that in the energy region $T_\pi < 800$ MeV [$E_{c.m.} < 1630$ MeV],

all partial waves with $J \leqslant 5/2$ have sizable inelasticities. On the other hand, the amplitudes for $J \geqslant 7/2$ are either elastic in this energy region, or are just about to start becoming slightly inelastic. In Fig. 6 the partial-wave inelastic cross sections

$$\sigma_{inel} = \pi\lambda^2 (J + 1/2)(1 - \eta^2) \tag{5}$$

(excluding elastic charge exchange) are shown for $J \leqslant 3/2$. The values of the elasticity parameters $\eta = |S^{(el)}_{J,\ell}|$ are taken from the analyses of elastic πN scattering by different groups. Except for $J^P = 3/2^+ (P_{13})$, these inelastic cross sections show resonance behavior. The well-established $I = 1/2$ resonances important for this energy region are listed in Table III.

For all of these resonances except $S_{11}(1550)$, the dominant "inelastic" (i.e., non-πN) decay channel is expected to be $\pi\pi N$, whereas for the $S_{11}(1550)$ resonance, this decay mode is probably unimportant, the dominant "inelastic" mode being ηN in this case (see Fig. 6).

From analysis of the inelastic reaction $\pi N \rightarrow \pi\pi N$, one hopes to

(i) separate the various reaction amplitudes according to their J^P values;

(ii) further separate, for each J^P, the different interfering decay channels such as $\pi\Delta$, "σ" N, or "ρ" N. (Here "σ" stands for an $I = 0$, S-wave $\pi\pi$ pair in an attractive but not necessarily resonant interaction, while "ρ" stands for a pion pair in the $I = 1$, P wave state with a mass below or around the rho meson resonance mass. Note that the 1704-MeV threshold for production of pion pairs with a mass of $m_\rho = 765$ MeV is at $T_\pi = 925$ MeV.)

In contrast to the partial-wave analysis of elastic πN scattering, the difficulty with three particles in the final state is that the complete partial-wave expansion is not unique. For a given overall J^P one may, for example, expand the amplitude into a series of terms labeled by the quantum numbers shown in Fig. 7(a). Using such an expansion [we call it the (12)3 expansion], one analyzes for definite angular momentum and isospin states of the (12) subsystem. Transition amplitudes into states with a definite angular momentum in, for example, the (23) subsystem however would, in the (12)3 expansion, in general be represented by a large number of terms, and would not be easily recognizable. To simplify the problem it is usually assumed that, for each of the three pairs of particles in the final state, one or a few simple sets of quantum numbers dominate, due to some strong two-body final-state interactions in certain angular momentum and isospin states. For each two-particle subsystem, in addition to the few states assumed to be enhanced by the final-state interactions in this pair, other states will in general be superimposed as a consequence of the final-state interactions in the other pairs. In this way, one arrives at an isobar model, with interactions in each of the pairs [Fig. 7(b)]. If one further specifies the dynamical form of the interactions in each of the pairs (by an energy-dependent two-particle scattering phase shift, or simply by a complex propagator or scattering length), one has a complete parameterization of the three-particle production amplitude at fixed total energy E. This may then be fitted to the experimental data.

The status of the phenomenology involved and the results from various attempts to analyze the published data on $\pi N \rightarrow \pi\pi N$ in the $I = 1/2$

state have been recently reviewed by Morgan.[7] First we discuss the methods, then the results.

Two different approaches have been used. The first of these, as described by Arnold and Uretsky,[11] is model-independent. One uses basically only information on the production angle distribution $d\sigma/d\Omega$, ignoring information on the specific properties of the decay of the intermediate state into the final $\pi\pi N$ state. One expands $d\sigma/d\Omega$ (which for a three-particle final state depends in general on two independent angles that can be specified in different ways[12]), into a series of, e.g., spherical harmonics:

$$d\sigma/d\Omega\,(\cos\Theta, \Phi) = \sum_{\ell, m} A_\ell^m Y_\ell^{m^*}(\Theta, \Phi); \qquad A_\ell^{-m} = (-)^m A_\ell^{m^*}.$$

The expansion coefficients A_ℓ^m can be expressed as a sum over contributions from the various bilinear combinations of amplitudes corresponding to different J^P, in complete analogy with the Legendre polynomial expansion of elastic scattering differential cross sections.[13] In particular, with the choice (a) of the production angles Θ, Φ as defined in footnote 12, and with M being the component of the total angular momentum $\vec{J}$ normal to the plane spanned by the three final-state c.m. momenta, the following rules apply:[14]

(1) There can only be terms with $\ell + m$ even.[12a]

(2) The interference between two partial waves with J, M and J', M' contributes only to A_ℓ^m with $|J - J'| \leq \ell \leq J + J'$ and $m = M - M'$.

(3) The absolute magnitude squared of a partial-wave amplitude of angular momentum J contributes to A_ℓ^m with even $\ell \leq 2J - 1$.

(4) The interference terms between two partial waves of even (odd)

relative parity contribute only to A_ℓ^m with ℓ = even (odd).

(5) The amplitude labeled by J, M corresponds to a transition in a state with parity $(-)^{M-\mu}$, where μ is the component of the spin of the final nucleon normal to the plane of the three final-state c.m. momenta.

This expansion then allows one easily to estimate the highest contributing angular momentum J_{max}, and, hopefully, to identify the behavior of particular partial waves from the behavior of those expansion coefficients to which these partial waves contribute. One can study the expansion coefficients (as a function of the total energy for example) either integrated over the Dalitz plot, or for individual regions of the Dalitz plot. Arnold and Uretsky[11] have used this method to check consistency of $\pi\pi N$ data with the inelasticity determinations as plotted in Fig. 6. Also Roberts[15] has used $d\sigma/d\Omega$ data restricted to the Δ band of the Dalitz plot and checked to see whether decay from the different J^P channels into just the $\pi\Delta$ configuration saturates the total inelasticity known from EPSA.

The second approach consists in fitting an isobar model,[16-19] that gives information on both (i) and (ii) above. Thurnauer,[17] Olsson and Yodh,[10] and Morgan,[7] analyzing the region $T_\pi \leq 800$ MeV, have used essentially similar models, in which the full amplitude is the sum of the three "isobar" amplitudes of Fig. 7(b). Their assumptions differ mainly in which partial-wave transitions they include. Olsson and Yodh[10] use $\pi\Delta$ and $\pi(\pi N)_{I=1/2,\ S\ wave}$ final states (i.e., they assume πN final-state interactions in $I = 1/2$, $J^P = 1/2^-$ "$(\pi N)_S$" and $I = 3/2$, $J^P = 3/2^+$ "Δ" states). Thurnauer[17] uses $\pi\Delta$ and "σ"N. Both assume only S-wave production of the "isobars." Their assumptions are not as different as

they might seem since there is very strong overlap between S-wave $\pi(\pi N)_S$ and "σ"N final states, in each case all three particles being in relative S waves.

Morgan[7] in addition considers "ρ"N states (the "ρ" being described by the tail of a resonance pole at 750 MeV), and adds P-wave production of the isobars.

As mentioned above, the final states considered in the isobar model in general belong to <u>different</u> complete orthogonal sets of states, corresponding to the different possible coupling schemes $(\pi_1\pi_2)N$, $\pi_1(\pi_2 N)$, or $\pi_2(\pi_1 N)$. Therefore, Namyslowski et al.[18] choose a somewhat different approach. They do not just add the three separate <u>complete</u> amplitudes, as given by the isobar model for transitions into these various final states. Instead, they project all final states onto a common set of complete states, say the one corresponding to the $(\pi_1\pi_2)N$ coupling scheme, and then only add the contributions, from the different terms of the isobar model, to the amplitudes for transition into the <u>few</u> <u>lowest</u> states of this set (i.e., just the ones whose presence is actually indicated by the experimental data). While this procedure is not much more complicated than the straight isobar model approach, Namyslowski et al. suggest that it is more systematic since one deals with just one set of amplitudes, defined in terms of one complete set of quantum numbers of the (initial and) final state.

Naturally, this approach can be extended beyond the isobar model. However, the present experimental data, entirely lacking in polarization measurements, leave the phase shift analyses badly underdetermined. Hence in the analysis at present one is forced to make simplifying

assumptions, which amounts to using an isobar model. Whether the Namyslowski et al. approach to the isobar model is a more economical description of what is going on in $\pi N \to \pi\pi N$, than the straight ("naive") isobar model, may soon be learned as more accurate data are subjected to phenomenological analysis.

Finally, one may, within the isobar model, use t and u channel exchange amplitudes to describe the contributions of the partial waves with higher J to isobar production in closed form (i.e., without having to introduce arbitrary parameters for each isobar production partial-wave amplitude). Thus, ρ exchange is expected to be important for $\pi N \to \pi\Delta$, and pion exchange for $\pi N \to \sigma N$ or $\pi N \to \rho N$.

The results from the published analyses are summarized in Fig. 8.

(i) P_{11}: This partial wave is strongly seen in the $\pi N \to \pi\pi N$ reaction above $T_\pi = 300$ MeV. All analyses agree that there is $P_{11} \to$ "σ"N, S-wave decay (which has 90% overlap[7] with $P_{11} \to \pi(\pi N)_{S\,wave}$, S wave, integrated over the Dalitz plot). In addition, there are indications for $P_{11} \to \pi\Delta$, P wave, and/or $P_{11} \to$ "ρ"N, P wave. For $T_\pi \geq 550$ MeV, Morgan's analysis[7] suggests a large $P_{11} \to$ "ρ"N, P-wave amplitude, possibly resonant. In fact the CERN analysis[20] of elastic πN scattering suggests a second, very broad P_{11} resonance at $E_{c.m.} = 1750$ MeV ($T_\pi = 1010$ MeV).

(ii) D_{13}: The inelastic decay of this resonance ($\Gamma_{in}/\Gamma_{tot} \approx 40\%$) is clearly established to be dominantly $D_{13} \to \pi\Delta$, S wave. Only Namyslowski et al.[18] assume an equally large contribution of $D_{13} \to \pi\Delta$, D wave which seems somewhat unplausible in view of the centrifugal barriers involved.

Morgan[7] finds in addition contribution from $D_{13} \rightarrow$ "σ"N, P wave.

(iii) Nothing is known yet about the magnitude and decay channels of the P_{13} and S_{11} into $\pi\pi N$. Also the decay modes of the D_{15} and F_{15} states (both resonant at $T_\pi \approx 900$ MeV) into $\pi\pi N$ have not yet been studied in detail. Roberts[15] finds very little (< 30%) $\pi\Delta$ final state, whereas Courau[21] fits the data with D_{15} and $F_{15} \rightarrow \pi\Delta$ plus ρ exchange leading to $\pi\Delta$; both authors, however, neglect interferences with other possible decay modes.

2. $I = 3/2$, $\pi N \rightarrow \pi\pi N$

(a) Threshold ($T_\pi = 270$ MeV) to $T_\pi = 820$ MeV The $\pi N \rightarrow \pi\pi N$ data in this region have been analyzed by Olsson and Yodh[10] and by Namyslowski et al.[18] Let us summarize their results and compare them with the results on inelasticities from the EPSA.

Olsson and Yodh make the most detailed fit to the data, using an isobar model. They find the dominant amplitude to be $D_{33} \rightarrow \pi\Delta$, S wave. To this they add a $P_{31} \rightarrow \pi(\pi N)_{I=1/2,\, S\ wave}$, S-wave amplitude to get the correct behavior of $\sigma(\pi^+ p \rightarrow \pi^+\pi^0 p)/\sigma(\pi^+ p \rightarrow \pi^+\pi^+ n)$. They choose this with the prejudice that S-wave states should dominate. To get the correct angular distributions in the $\pi^+\pi^0 p$ channel, they have to add another amplitude from the same initial state, $P_{31} \rightarrow \pi\Delta$, P wave, as a "background term" (corresponding to about 10% contribution to $\sigma(\pi^+ p \rightarrow \pi^+\pi^0 p)$ at $T_\pi = 600$ MeV). The phases and magnitudes of all three amplitudes are assumed independent of the total c.m. energy. The phases are relatively real, with the two P_{31} amplitudes being negative relative to the D_{33} amplitude. It is claimed that this model agrees with all the data available until 1966 below $T_\pi = 800$ MeV.

Namyslowski et al.,[18] on the other hand, compare with data at $T_\pi = 600$ MeV and $T_\pi = 820$ MeV only. They do not claim complete agreement; the worst discrepancy is with production angular distributions (where interferences between amplitudes for different J^P show up). In fact, their fits at $T_\pi = 600$ MeV to the angular distributions of the p and the π^0 in $\pi^+ p \to \pi^+ \pi^0 p$ are not as good as those of Yodh and Olsson.[10] They assume, at $T_\pi = 600$ MeV, a superposition of $D_{33} \to \pi\Delta$, S and D wave, and $S_{31} \to \pi\Delta$, D wave. At $T_\pi = 820$ MeV, they again take $D_{33} \to \pi\Delta$, S and D wave, but instead of S_{31}, they now add $P_{33} \to \pi\Delta$, P and F waves. They find that any inclusion of S_{31} destroys the fit at this energy.

Looking at the I = 3/2 elasticity parameters η from the EPSA[20, 23, 24] one finds the following values:

		η (as defined in Fig. 5)					
T_π (MeV)	$\sqrt{s}$ (MeV)	S_{31}	P_{31}	P_{33}	D_{33}	D_{35}	F_{35}
600	1512	0.9	1 - 0.9	≈0.95	0.9	1	1
820	1643	0.4(res.)	1 - 0.8	≈0.8(res?)	0.7(res?)	0.8 - .95	≈0.9

For all the other partial waves, $\eta = 1$ in the energy region in question.

In one[20] of the EPSA, one finds $\eta(P_{31}) = 1$ for $T_\pi < 600$ MeV, which would be inconsistent with a sizable P_{31} contribution to $\pi N \to \pi\pi N$ in $T_\pi \leq 600$ MeV, as assumed by Yodh and Olsson.[10] It is well known, however, that the S_{31} amplitude goes through an inelastic resonance ($\eta = 0.4$) at $T_\pi = 820$ MeV, and P_{33} probably resonates at $T_\pi = 900$ MeV ($\eta = 0.7$). Therefore, one would expect to find a contribution from these partial waves in the $\pi N \to \pi\pi N$ channel. Regarding the Namyslowski et al.[18]

analysis, it seems hard to understand that S_{31} should contribute at $T_\pi = 600$ MeV (i.e., below resonance), but not at the resonance itself where the inelasticity is largest.

(b) $T_\pi = 820 - 1300$ MeV No detailed analysis has been reported in the literature. Only the production angular distributions have been discussed, and sometimes the analysis is restricted to $\pi\Delta$ final states. This selection becomes possible at these energies since the overlap region of the two Δ bands moves outside the Dalitz plot. However, as the energy increases, ρ production has to be taken into account (> 10% for T > 1000 MeV).[6]

Kraybill et al.[6] expand the differential cross section for $\pi^+ p \to \pi^0 \Delta^{++}$ into a series of P_ℓ (cos θ) up to $\ell = 7$; they find no evidence for higher terms in this energy region. Deler et al.[22] choose a more general method, expanding the production angular distribution $d\sigma/d\Omega$ (cos Θ, Φ) for $\pi^+ p \to \pi^+ \pi^0 p$ into a series of spherical harmonics $Y_\ell^m(\theta, \Phi)$. In both papers the expansion coefficients are then compared with theoretical expressions from a simple $\pi N \to \pi\Delta$ isobar model. The results are summarized below.

In the $T_\pi \approx 800$ MeV region, the presence of $P_{33} \to \pi\Delta$, P wave, and $D_{35} \to \pi\Delta$, D wave, are indicated, but other amplitudes are present as well. No firm conclusion is reached about the S_{31}, D_{33}, and P_{31} amplitudes, which are also expected to contribute. From the elastic phase shift analysis, P_{33} is known to probably resonate, and D_{35} to have already a sizable inelasticity ($\eta = 0.95$ from the CERN,[20] $\eta = 0.8$ from the Saclay[23] phase shift analysis) in this energy region.

In the interval between $T_\pi = 900$ and 1200 MeV, the $F_{37} \rightarrow \pi\Delta$, F-wave amplitude seems to begin showing up, interfering with the $J^P = 1/2^\pm$, $3/2^\pm$ amplitudes.

(c) Finally for the $T_\pi \approx 1300$ MeV region ($E_{c.m.} \approx 1900$ MeV), the results are compatible with dominance of $F_{37} \rightarrow \pi\Delta$, F wave, which is near resonance there ($\eta \sim 0.4$). There could also be a $F_{35} \rightarrow \pi\Delta$, F-wave amplitude interfering with it; from the elastic scattering phase shift analysis, F_{35} is known to probably resonate at $T_\pi = 1330$ MeV with $\eta = 0.7$. However, no conclusion is possible about the size of the F_{35} amplitude from the inelastic reaction with the present data and analysis. The presence of further amplitudes of the same parity is indicated in the inelastic production angular distributions; these might be $P_{33} \rightarrow \pi\Delta$, P wave (which, however, has only $\eta \sim 0.9$ at this energy), or $P_{31} \rightarrow \pi\Delta$, P wave (which actually probably resonates[20] at $T_\pi = 1375$ MeV with $\eta \sim 0.4$). In addition, there seem to be some indications for the presence of amplitudes for negative parity also. The $D_{35} \rightarrow \pi\Delta$, D-wave amplitude seems to decrease above $T_\pi = 1000$ MeV and is found to be absent at $T_\pi = 1300$ MeV, although from the elastic scattering analysis its η is decreasing monotonically, with $\eta \approx 0.5$-0.7 at $T_\pi = 1300$ MeV, reaching a possible resonance at $T_\pi \approx 1400$ MeV (with $\Gamma \sim 310$ MeV according to the CERN EPSA[20]). These two considerations lead one to conclude that the D-wave $\pi\Delta$ decay of this resonance (if it exists) must be very small.

It might be mentioned that Courau[21] gets a rather satisfactory fit to the π^0 angular distribution in $\pi^+ p \rightarrow \pi^+ \pi^0 p$ at $T_\pi = 1300$ MeV, using only a resonating $F_{37} \rightarrow \pi\Delta$, F-wave amplitude and adding a term in the cross section that describes non-interfering Δ production via ρ exchange.

3. Other Channels: $\pi^- p \to \eta N$, $K\Lambda$ $(I = 1/2)$

(a) $\pi N \to \eta N$

For the $1/2^-$ (S_{11}) partial wave we have already shown in Fig. 6 that $\sigma_{inel}(1/2^-)$ as determined from EPSA is within the errors accounted for by the sudden increase from threshold of $\sigma(\pi N \to \eta N)$. At the top of Fig. 9 we show the actual data[25] for $\sigma(\pi^- p \to \eta n)$, compared with $\sigma_{inel}(1/2^-)$ as predicted by various EPSA's. Then below are the partial cross sections, A_ℓ, for the expansion $d\sigma/d\Omega = \Sigma A_\ell P_\ell(\cos\theta)$.

Below $T_\pi = 1000$ MeV ($E_{c.m.} = 1745$ MeV) only A_0, A_1, A_2 are different from zero. Besides S_{11}, other partial waves must be present; a combination of S_{11}, P_{11}, and D_{13} actually can explain the data[25] (although, by the Minami ambiguity, D_{13} could be replaced by P_{13}). At $T_\pi = 900$ MeV ($E_{c.m.} = 1688$ MeV) the $5/2^-$ (D_{15}) and $5/2^+$ (F_{15}) amplitudes are known to resonate and to be highly absorptive; nevertheless, no enhancement in $\sigma(\pi^- p \to \eta n)$ and no A_3, A_4 expansion coefficients are observed at this energy, which means that the relative decay rate into ηN of these resonances must be quite small (<2.5% and <1.5%, respectively[30]).

It has been pointed out[25a] that the η production data are also quite consistent with the peak in $\sigma(\pi N \to \eta N)$ near threshold being dominated by a (new) P_{11} resonance at $E_{c.m.} = 1580$ MeV ($\Gamma = 130$ MeV, decay rate $\to \pi N$ 35%; $\to \eta N$ 30%), which must then be different from the well-established P_{11} resonance at $E_{c.m.} = 1470$ MeV. In the EPSA's,[20,23,24] no indication of such a resonance is seen; however, it seems that its existence can at present not be excluded on the basis of the elastic data alone. Measurement of the recoil nucleon polarization could resolve this ambiguity in the η production data.

(b) $\pi N \to K\Lambda$

Cross-section and angular distribution data[26] for $\pi^- p \to K^0\Lambda$ between threshold (at $E_{c.m.} = 1615$ MeV) and $E_{c.m.} = 1750$ MeV are shown in Fig. 10. The large values of the A_1, A_2, and A_3 coefficients in the Legendre polynomial expansion of $d\sigma/d\Omega$ indicate considerable interference between at least two partial-wave amplitudes of different parity; from the absence of significant A_4 and A_5 coefficients at $E_{c.m.} \approx 1680$ MeV it appears, however, that the contributions from the resonant D_{15} (1680) and F_{15} (1688) partial waves to the $K\Lambda$ channel are small. Upper limits on the $K\Lambda$ decay branching ratios of these resonances, as inferred[30] from the experimental limits on A_4 and A_5, are given in Table IV. Further analysis of these data is in progress.[26]

III. SIGNS AND MAGNITUDES OF INELASTIC AMPLITUDES, SU(3) ASSIGNMENTS

We have already suggested that successes in K^-p experiments may predict a bright future for πp studies. Figure 11 shows another sort of K^-p result,[27] this time unique to inelastic channels. It shows Argand plots for $Y^* \to \pi\Sigma$; we recognize resonant circles for two cases with $J^P = 3/2^-$, $\Lambda(1690)$ and $\Sigma(1660)$ and for two more $5/2^+$ cases, $\Lambda(1815)$, $\Sigma(1910)$. The point we want to illustrate here is that two of the curves are plotted "up" (i.e., with +i components) and two "down," i.e., the signs of the partial-wave amplitudes have been determined from the experimental angular distributions.

Let us pursue further the significance of these signs. Consider two final-state amplitudes of some resonance Y^*, produced by K^-p:

$$K^-p \xrightarrow{g_{K^-p}} Y^* \xrightarrow{g_{K^-p}} K^-p; \ \langle K^-p|T^{JP}|K^-p\rangle \propto g^2_{K^-p}; \tag{6}$$

positive definite

$$K^-p \xrightarrow{g_{K^-p}} Y^* \xrightarrow{g_{\pi\Sigma}} \pi\Sigma; \ \langle \pi\Sigma|T^{JP}|K^-p\rangle \propto g_{K^-p}\, g_{\pi\Sigma} = \pm|g_{K^-p}\, g_{\pi\Sigma}|. \tag{7}$$

In the first case (elastic scattering), the initial and final coupling constants are the same, and the partial-wave amplitude is necessarily positive. In the second (inelastic) case, we introduce a new coupling constant $g_{\pi\Sigma}$, and until we invoke SU(3), all we know is that it is real. Of course we cannot even measure the sign of the amplitude until we let it interfere with another partial wave. But fortunately there are other resonances close enough in energy so that their two $\pi\Sigma$ modes overlap, and with adequate data the CERN-Heidelberg-Saclay group[27] has determined the relative signs, as shown in Fig. 11. Other determinations have been made by Kernan and Smart, who were among the first to study these signs.[28]

In the language of SU(3), however, the sign of the amplitude ($\pi\Sigma$ in Eq. 7) is no longer unknown, since there is of course only <u>one</u> real coupling constant g for reactions such as $Y^* \to 8 \otimes 1$ or $8 \otimes 10$. For the particular (but most common) case that Y^* is itself a member of an 8, and decays into $8 \otimes 8$, there can actually be two g's (although frequently one of them is zero); but even here, as we shall describe below, given a little additional data, the sign of the final amplitude is predicted and is a check on the SU(3) assignment of the resonance Y^*. Further, though magnitudes may be hard to measure, signs are easier.

In fact, about 10 such signs have now been reported, 8 of which afford significant tests. The chance that some random SU(3) assignment would pass all 8 tests is then only 2^{-8}, so we see how valuable these signs can be.

To illustrate further the question of making SU(3) assignments to the experimental data, we introduce Table IV and Fig. 12, both taken from Tripp et al.[30]

Note that Table IV is very weak on N^* and Δ inelastic branching fractions; it lists two ηN fractions, two ηN upper limits, and two $K\Lambda$ upper limits. With that limited information we conclude our N^* discussion; the rest of this section is only a summary of the status of SU(3) assignments and a hint as to how better N^* data may be used in the future.

Table IV lists two possible 10's: the $3/2^+$ supermultiplet has three members whose branching fractions are related by SU(3), the $7/2^+$ has two. In their Letter,[30] they show that the decay rates are compatible with the predictions of SU(3) to within $\pm 30\%$. In addition, two singlet assignments [for $\Lambda(1520)$ and $\Lambda(2100)$] fit well if one allows for some singlet-octet mixing.

Finally Table IV lists four possible octets. Here, because of the complications that $8 \otimes 8$ couples to <u>two</u> 8's (one symmetric, 8_s, one antisymmetric, 8_a), the checking is not so straightforward. Tripp et al.[30] do it in an interesting graphical way in their Fig. 3, which is our Fig. 12. Since they had little room in their paper to explain their treatment of signs, we will expand on it here.

Since all the data are treated as partial widths, assume the resonance has been created with unit amplitude. For definiteness, call the decaying resonance Y^*, and remember it is part 8_s and part 8_a. Write the partial width Γ as

$$\Gamma = (c_s\, g_s + c_a\, g_a)^2 \times \text{Kinematics}, \tag{8}$$

where Kinematics stands for all kinematical and phase space factors, including barrier penetration factors B_ℓ for orbital angular momentum ℓ, i.e.,

$$\text{Kinematics} = B_\ell\,(p)\left(\frac{M_N}{M_Y^*}\right)p,$$

and where c_s, c_a are isoscalar coefficients, thus for $\bar{K}N$,

$$\Gamma\,(\bar{K}N) = [c_s\,(\bar{K}N)g_s + c_a\,(\bar{K}N)g_a]^2 \times \text{Kinematics}.$$

The square root of (8) yields an amplitude $A\,(\bar{K}N, \pi\Sigma, \cdots)$ as

$$A = c_s\, g_s + c_a\, g_a = \pm\sqrt{\Gamma/\text{Kinematics}}.$$

If we plot $g_a \equiv y$ versus $g_s \equiv x$, we get straight lines,

$$y_\pm = \frac{\pm|A| - c_s x}{c_a}\ . \tag{9}$$

Note that the greater the observed amplitude $|A|$ $(\propto \sqrt{\Gamma})$, the farther the two lines $y_\pm$ lie from the origin.

Since one overall sign is always undetermined, we chose $x = g_s$ to be > 0, and plot only the right half plane. Satisfactory agreement among members of an octet is indicated by a common value of x and y for all decay modes. Shaded areas indicate where the lines cross. Tripp et al. discuss all four octets in turn, but we can see that for each octet the lines overlap within errors with one serious discrepancy in each case.

Finally we come to the question of the signs, which are shown in Fig. 12 as dashed lines with arrows indicating allowed regions. Figure 13 illustrates how some of these areas were constructed, using the fact of Fig. 11 that in the $3/2^-$ octet the I = 0 and I = 1 $\pi\Sigma$ amplitudes are found to be of opposite sign.

Figure 13(a) shows the straight lines $y_\pm$ ($\bar{K}N$) from Eq. (9); y_+ is labeled (+), etc. For the $\pi\Sigma$ decay mode, $c_a = 0$, giving vertical lines, $x_\pm = \pm |A|/c_s$, only one of which, x_-, is in the right half plane (since c_s happens to be $-\sqrt{15/5}$). The line is labeled (-). Since the reaction under discussion is $\bar{K}N \rightarrow Y^* \rightarrow \pi\Sigma$, the sign of $|\pi\Sigma\rangle$ is of course the sign of the product of $|\bar{K}N\rangle$ and $|\pi\Sigma\rangle$. We have written these products inside circles where the $\bar{K}N$ and $\pi\Sigma$ lines cross. The whole plane is then seen to be divided into four sectors, two of them $\ominus$ (shaded), and two of them $\oplus$ (unshaded).

Figure 13(b) repeats the reasoning for I = 1. Here the only difference is that for the $\pi\Sigma$ decay, it is c_s which is zero, so we find horizontal lines. Since we want the signs of the I = 0 and I = 1, $\pi\Sigma$ amplitudes to be opposite, as found experimentally, we shade the $\oplus$ sectors this time.

The allowed solution must then fall in a sector where there is shading for both i-spin states, or for neither. For our example Fig. 13(c) shows there is no unshaded overlap, so that only the doubly shaded overlap sectors are allowed. Fortunately the region of intersection of the lines, arrived at without sign considerations, falls in the upper overlap sector!

FOOTNOTES AND REFERENCES

*On leave from University of Hamburg.

1. G. Cocconi et al., Phys. Letters 8, 134 (1964); S. L. Adelman et al., Phys. Rev. Letters 13, 555 (1964); C. M. Ankenbrandt et al., Nuovo Cimento 35, 1052 (1965); C. Bellettini et al., Phys. Letters 18, 167 (1965); E. W. Anderson et al., Phys. Rev. Letters 16, 855 (1966); I. M. Blair et al., Phys. Rev. Letters 17, 789 (1966); E. Gellert et al., Phys. Rev. Letters 17, 884 (1966); S. Almeida et al., Nuovo Cimento 50A, 1000 (1967); K. J. Foley et al., Phys. Rev. Letters 19, 397 (1967); V. Alles-Borelli et al., Nuovo Cimento 47, 232 (1967); G. Alexander et al., Phys. Rev. 154, 1284 (1967); Y. Y. Lee et al., Phys. Rev. 159, 1156 (1967). See also the Review by Van Hove, Proceedings XIIIth International Conference on High Energy Physics, Berkeley (1967), p. 253; and A. H. Rosenfeld et al., Rev. Mod. Phys. 40, 77 (1968).
2. G. Goldhaber, Proceedings 1967 Coral Gables Conference, p. 190.
3. E. L. Berger, E. Gellert, G. A. Smith, E. Colton, and P. Schlein, Lawrence Radiation Laboratory Report UCRL-18110, Feb. 1968 (unpublished).
4. M. N. Focacci and G. Giacomelli, Pion Proton Elastic Scattering; CERN 66-18 (1966), unpublished.
5. J. P. Merlo and G. Valladas, Proc. Roy. Soc. (London) 289A, 489 (1966).
6. H. L. Kraybill, D. L. Stonehill, B. Deler, W. Laskar, J. P. Merlo, G. Valladas, and G. W. Tautfest, Phys. Rev. Letters 16,

863 (1966). This paper contains also a list of other references used in preparing Fig. 3. See also the references given in Table II.

7. D. Morgan, Phys. Rev. 166, 1731 (1968). (For the individual references on the data of Fig. 4, see also Tables I and II.)

8. R. D. Tripp, Proceedings of the International School of Physics "Enrico Fermi," Course XXXIII, p. 70 (1966).

9. R. M. Sternheimer and S. J. Lindenbaum, Phys. Rev. 105, 1874 (1957); 106, 1107 (1957); 110, 1723 (1958); 123, 333 (1961).

10. M. G. Olsson and G. B. Yodh, Phys. Rev. 145, 1309 (1966); G. B. Yodh and M. G. Olsson, Phys. Rev. 145, 1327 (1966).

11. R. C. Arnold and J. L. Uretsky, Phys. Rev. 153, 1443 (1967).

12. These angles could be specified as described at the beginning of this section; however, for the present application it is more convenient to define them as the polar angles Θ, Φ of the incoming beam direction in a coordinate system fixed with respect to the three final-state particles, in the overall c.m. system. Two popular choices of the axes are: (a) z axis along the normal to the 3-particle decay plane, x axis in the 3-particle plane (e.g., along one of the momenta $\vec{p}_i$, or such that it bisects the angle between $\vec{p}_j$ and $\vec{p}_k$); (b) z axis along one of the final state momenta $\vec{p}_i$, x axis perpendicular to the 3-particle decay plane.

12a. Remember that the symmetry about the equator of $Y_\ell^m(\Theta, \Phi)$ is $(-)^{\ell+m}$. To see that this symmetry must be even, note that $\cos\Theta = \hat{\underline{n}} \cdot \hat{\underline{p}}$ [between normal (an axial vector) and beam (a vector)] is of course a pseudoscalar and must have zero expectation value. Hence $d\sigma/d\Omega$ must be symmetric about the equator,

and every Y_ℓ^m in its expansion must have $\ell + m$ even.

13. See, for example, R. D. Tripp, Ann. Rev. Nucl. Sci. 15, 325 (1965).

14. More details may be found in Reference 7, and in L. R. Miller and P. H. Söding, Production Angular Distributions of 3-body final states, Alvarez Group Physics Note No. 652, where a table of the A_ℓ^m in terms of the partial-wave amplitudes is given.

15. R. G. Roberts, Ann. Phys. 44, 325 (1967).

16. The theoretical foundation for a relativistic isobar model, using the Fadeev-Lovelace theory of composite particle scattering, has been given by D. Z. Freedman, C. Lovelace, and J. M. Namyslowski, Nuovo Cimento 43A, 258 (1966). Relativistic formulations of the isobar model have been described and compared with experimental data, in references 17-19.

17. P. G. Thurnauer, Phys. Rev. Letters 14, 985 (1965); Relativistic Analysis of Scattering Reactions with 3-Body Final States, Univ. of Rochester Report No. UR-875-119 (1966), unpublished.

18. J. M. Namyslowski, M. S. K. Razmi, and R. G. Roberts, Phys. Rev. 157, 1328 (1967).

19. B. Deler and G. Valladas, Nuovo Cimento 45A, 559 (1967); and private communication.

20. C. Lovelace, Rapporteur's talk, Proceedings of the 1967 Heidelberg Conference on Elementary Particles, to be published.

21. A. Courau, Nuovo Cimento 46A, 291 (1966).

22. B. Deler, J. P. Merlo, G. W. Tautfest, and G. Valladas, paper submitted to the XIIIth International Conference on High Energy

Physics at Berkeley (1966), unpublished.

23. P. Bareyre, C. Bricman, and G. Villet, Phys. Rev. 165, 1730 (1968).

24. C. H. Johnson, Lawrence Radiation Laboratory Report UCRL-17683, Aug. 1967 (unpublished); H. M. Steiner, invited talk at this conference.

25. W. B. Richards, C. B. Chiu, R. D. Eandi, A. C. Helmholz, R. W. Kenney, B. J. Moyer, J. A. Poirier, R. J. Cence, V. Z. Peterson, N. K. Sehgal, and V. J. Stenger, Phys. Rev. Letters 16, 1221 (1966); W. B. Richards, Lawrence Radiation Laboratory Report UCRL-16195, Nov. 1965 (unpublished).

25a. S. Sasaki, J. Takahashi, and K. Ozaki, Prog. Theor. Phys. 38, 1326 (1967).

26. J. Anderson, F. S. Crawford, and J. Doyle, private communication; J. Doyle, Lawrence Radiation Laboratory Report UCRL-18139, 1968 (unpublished).

27. R. Armenteros, M. Ferro-Luzzi, D. W. G. Leith, R. Levi-Setti, A. Minten, R. D. Tripp, H. Filthuth, V. Hepp, E. Kluge, H. Schneider, R. Barloutaud, P. Granet, J. Meyer, and J. P. Porte, Phys. Letters 24B, 198 (1967).

28. A. Kernan and W. Smart, Phys. Rev. Letters 17, 832; 1125 (E) (1966), see also A. H. Rosenfeld, Proc. 1966 Yalta School of Elementary Particles, p. 153.

29. J. J. de Swart, Rev. Mod. Phys. 35, 916 (1963).

30. R. D. Tripp, D. W. G. Leith, A. Minten, R. Armenteros, M. Ferro-Luzzi, R. Levi-Setti, H. Filthuth, V. Hepp, E. Kluge,

H. Schneider, R. Barloutaud, P. Granet, J. Meyer, and J. P. Porte, Nucl. Phys. B3, 10 (1967).

Table I. Some $\pi^- p$ inelastic hydrogen bubble chamber experiments. (Numbers of events enclosed in parentheses indicate experiments still in progress; for other comments, see text.)

$\pi^- p \rightarrow \pi\pi N$

$\sqrt{s}$ (MeV)		T_π (MeV)	No. events of $\pi^-\pi^0 p$	No. events of $\pi^+\pi^- n$	Reference
1305		290		250	Batusov et al., JETP 13, 320 ('61)
		330		(3500)	Oxford (145 K pictures taken)
	LRL SLAC	360		573	Kirz et al., PR 130, 2481 ('63)
		370		(3000)	Oxford (60 K pictures taken)
1390		410	(500)	(1600)	Saclay (60 K pictures taken)
		420		(4500)	Oxford
1400		430		450	Kirz et al., PR 130, 2481 ('63)
1416	↓	450	100	325	Poirier et al., PR 148, 1311 ('66)
	2K→	460		450	Kirz et al., PR 130, 2481 ('63)
		480		329	Kirz et al., PR 130, 2481 ('63)
1450		490	(1800)	(5000)	Saclay (60 K pictures taken)
1450		500	(1500)	(4000)	Oxford (50 K pictures taken)
1480		550	(2300)	(3800)	Saclay
		555		450	Kirz et al., PR 130, 2481 ('63)
		558	441	833	Burnstein et al., PR 137, B1044 ('65)
	2K→	604	1359	1970	Vittitoe et al., PR 135, B232 ('64)
		605		450	Kirz et al., PR 130, 2481 ('63)
		646	1049	1609	Oliver et al., PR 147, 932 ('66)
1525		620	(3600)	(5000)	Saclay (60 K pictures taken)
		650	538	777	Femino et al., NC 52A, 892 ('67)
		673		450	Kirz et al., PR 130, 2481 ('63)
	2K→	765	897	560	Crittenden et al., Sienna I, p. 116 ('63)
	2K→	775	833	1600	Bertanza et al., NC 44A, 712 ('66)
		780		450	Kirz et al., PR 130, 2481 ('63)
		790	466	942	Cason et al., PR 150, 1134 ('66)
		800	~200	~300	Gensollen et al., Sienna I, p. 84 ('63)
	2K→				
	2K→				
	2K→	830	414	881	Cason et al., PR 150, 1134 ('66)
	2K→				
	2K→	870	493	997	Cason et al., PR 150, 1134 ('66)
1688	2K→	900	671	1183	Gensollen et al., Sienna I, p. 84 ('63)
	2K→				
	2K→	905	216	354	Pickup et al., PR 132, 1819 ('63)
	2K→	960	262	384	Pickup et al., PR 132, 1819 ('63)
1800		1100	263	436	Pickup et al., PR 132, 1819 ('63)
		1100	(15 000)		Manning, Smith (LRL, '68 to be publ.) (from $\pi^+ d \rightarrow pp\pi^+\pi^-$)
2300		2200	(25 000)		LRL SLAC (Total LRL-SLAC, ~50 000 inelastic events spread over a $\sqrt{s}$ range of 500 MeV, so ~2000 events every 20 MeV.)
Total analyzed:			~8000	~15 000	

$\pi^- p \rightarrow K^0 \Lambda$

1613	768 = threshold			
1688	900	(8500)		Anderson, Crawford, Doyle (LRL)

Table II. Some π^+p inelastic hydrogen bubble chamber experiments.

$\pi^+p \to \pi\pi N$ T = 180 MeV (threshold) to 1100 MeV				
$\sqrt{s}$ (MeV)	T_π (MeV)	Events in channel $\pi^+\pi^0p$	$\pi^+\pi^+n$	Reference
	357		213	Kirz et al., PR 126, 763 ('62)
1415	450	100	28	Poirier et al., PR 148, 1311 ('66)
	500	159	40	Debaisieux et al., NP 63, 273 ('65)
1510	600	418	75	Newcomb et al., PR 132, 1283 ('63)
	810	2200		Deler et al., to be published
	820	346	73	Barlouland et al., NC 27, 238 ('63)
1690	900	274	75	Barlouland et al., NC 27, 238 ('63)
	900	274	201	Gensollen et al., Sienna I, p. 84 ('63)
	900	2517	529	Metzger et al., UR-875-186
	910	846	209	Stonehill et al., RMP 34, 503 ('62)
	980	4105		Tautfest and Willmann, Athens (Ohio), p. 421 ('65)
1760	1050	315	80	Barlouland et al., NC 27, 238 ('63)
	1090	951	249	Stonehill et al., RMP 34, 503 ('62)
	1130	3860		Tautfest and Willmann, Athens (Ohio), p. 421 ('65)
	1260	1365	490	Stonehill et al., RMP 34, 503 ('62)
1900	1300	3200		Deler et al., to be published (Saclay)
	1460	3150	1194	Daronian et al., NC 41A, 503 ('66)
	420 to 1070	$\frac{d\sigma}{d\omega}$ (π^0) only, counters. Detoeuf ('66)		
$\pi^+p \to K\Sigma$				
1690	900 =	threshold		
1851	1207	(500)		Birge, Borreani, Kalmus, LRL ('68)
1896	1297	(700)		Birge, Borreani, Kalmus, LRL
2015	1546	(700)		Birge, Borreani, Kalmus, LRL

Table III. Well-established $N^*_{1/2}$ resonances. with mass < 1700 MeV.

J^P	$\frac{1}{2}^+$ (P_{11})	$\frac{1}{2}^-$ (S_{11})		$\frac{3}{2}^-$ (D_{13})	$\frac{5}{2}^-$ (D_{15})	$\frac{5}{2}^+$ (F_{15})
Mass (MeV)	1470	1550	1710	1525	1680	1690
T_π (MeV)	530	660	940	620	880	900
Γ_{mass} (MeV)	210	130	300	115	170	130
$\Gamma_{T\pi}$ (MeV)	320	220	550	190	300	230
σ_{inel} (mb)	6	~4[a]	1.8	~7	10	10
η (see Fig. 5)	0.35	~0.4	0.7	~0.2	0.2	0.2
Γ_{el}/Γ_{tot}	0.66	0.33	0.79	0.57	0.39	0.68

[a]Mainly η production.

Table IV. Branching fractions and partial widths for baryon* → 8 ⊗ 8 (from Ref. 30).

Mass and width	Mode	Branching fraction	Partial Γ
$J^P = \frac{1}{2}^-$			
Λ(1405)	Σπ	1.0	35
N(1570)	Nπ	0.3	39
Γ = 130	Nη	0.7	91
Λ(1670) a)	NK̄	0.06	1.1
Γ = 18	Λη	0.94	16.9
$J^P = \frac{3}{2}^+$			
Δ(1236)	Nπ	1.0	120
Σ(1385) b)	Λπ	0.86	30.1
Γ = 35	Σπ	0.14	4.9
Ξ(1530)	Ξπ	1.0	7.3
$J^P = \frac{3}{2}^-$			
N(1530) i)	Nπ	0.65	68
Γ = 105	Nη		0.4
Σ(1660) c)	Λπ	0.10	5.0
Γ = 50	Σπ	0.67	33.5
	NK̄	0.10	5.0
Λ(1690) d)	Σπ	0.46	18.4
Γ = 40	NK̄	0.245	9.8
	Λη	< 0.027	< 1.1
Ξ(1815) e)	Ξπ	0.10	1.6
Γ = 16	ΛK̄	0.65	10.4
	ΣK̄	< 0.02	< 0.3
Λ(1520) j)	Σπ	0.51	8.2
Γ = 16	NK̄	0.39	6.2
$J^P = \frac{5}{2}^+$			
N(1688) f)	Nπ	0.65	71.5
Γ = 110	ΛK̄	< 0.0013	< 0.15
	Nη	< 0.015	< 1.7
Λ(1820) g)	Σπ	0.12	10.2
Γ = 85	NK̄	0.60	51
	Λη	< 0.014	< 1.15
Σ(1910) g)	Λπ	0.10	6
Γ = 60	Σπ	< 0.01	< 0.6
	NK̄	0.08	4.8
$J^P = \frac{5}{2}^-$			
N(1688) f)	Nπ	0.40	56
Γ = 140	ΛK	< 0.016	< 2.3
	Nη	< 0.025	< 3.5
Σ(1765)	Λπ	0.17	15.3
Γ = 90	Σπ	0.01	0.9
	NK̄	0.50	45
	Ση	< 0.005	< 0.5
Λ(1827) g)	Σπ	0.23	17.2
Γ = 75	NK̄	0.10	7.5
	Λη	< 0.08	< 6.1
Ξ(1933)	Ξπ	0.5	70
Γ = 140	ΛK̄	0.5	70
$J^P = \frac{7}{2}^+$			
Δ(1920)	Nπ	0.5	100
Σ(2035) h)	Λπ	0.25	40
Γ = 160	Σπ	0.06	9.6
	NK̄	0.16	25.6
	ΞK	< 0.016	< 2.6
$J^P = \frac{7}{2}^-$			
Λ(2100) h)	Σπ	0.05	8.0
Γ = 160	NK̄	0.29	46.4
	ΞK	0.01	1.6
	Λη	< 0.03	< 4.8

Footnotes

a) Branching fractions obtained on the two-channel assumption.
b) Width and branching fractions from ref. [9].
c) We adopt slightly higher elasticity than that reported in ref. [2]. Even so, there is insufficient Σ(1660) formed to accomodate the large Σπ amplitude required by the analysis of ref. [3] and in addition a comparably large rate into Λ(1405)π.
d) Branching fractions for Σπ and NK̄ from refs. [2,3]. The upper limit for Λη comes from the measured cross section of 0.08 mb at $\frac{1}{2}\Gamma$ above resonance as reported by Berley et al. [16].
e) Upper limit on the ΣK̄ mode is extracted from table 1 of the paper of Smith et al. [17] by comparison of the ΣK̄K and ΛK̄K reactions.
f) The upper limits on the decay mode N(1688) → ΛK were extracted from the unpublished associated production data of Anderson et al. [18]. The limits come from the absence of both A_4 and A_5 coefficients in the angular distributions of $\pi^- p \to \Lambda K^0$ in this momentum region. The coefficient A_5 is the more sensitive measure, and under the assumption that the two degenerate resonances of $J^P = \frac{5}{2}^-$ decay into ΛK in proportion to their probabilities of formation and to their respective centrifugal barriers, we obtain the limits listed. This ignores SU(3) as a starting value. Fig. 3cd shows that another iteration keeping A_5 fixed would satisfy SU(3). The upper limit on N → Nη comes from assigning a maximum enhancement of 0.3 mb to the reaction $\pi^- p \to N\eta$ at 1688 MeV as derived from the work of Richards et al. [19].
g) The Σπ and NK̄ rates are from refs. [1-3]. The upper limits on the Λη rates for Λ(1820) and Λ(1827) are obtained from the measured cross section of 0.2 mb.
h) Preliminary estimate of the Σπ mode from Barbaro-Galtieri [20]. The ΞK mode is estimated from the cross section for $K^- p \to \Xi K$ reported by Berge et al. [21]; the Λη upper limit is from Flatté and Wohl [21].
i) Nη partial width from the analysis of Davies and Moorhouse [22].
j) A more recent compilation by Yodh [23] gives for Λ(1520) a lower branching ratio Γ(Σπ)/Γ(NK̄) = 0.42/0.47, which indicates a greater need for singlet-octet mixing than shown in fig. 1.

FIGURE CAPTIONS

Fig. 1. $\pi^- p$ cross sections. σ_{tot} and σ_{el} are from Ref. 4, $\sigma_{\pi\pi N}$ is from Ref. 5. The insert (fraction in Δ bands), from Ref. 5, is described in the text. For references on $\sigma_{\pi\pi\pi N}$, see Table I. Smooth curves have been drawn through the measured points.

Fig. 2. Dalitz plot of ~2000 events of the reaction $\pi^- p \rightarrow \pi^+ \pi^- n$ at $T_\pi = 900$ MeV ($\sqrt{s} = 1688$ MeV). From LRL-SLAC collaboration (unpublished).

Fig. 3. $\pi^+ p$ cross sections (Ref. 6).

Fig. 4. Cross section for $\pi^\mp p \rightarrow \pi\pi N$, five charge states. Taken mainly from Ref. 7. The solid curves are the results of the fit of Olsson and Yodh, Ref. 10, as discussed in Section II.

Fig. 5. Argand plot for the elastic scattering amplitude.

Fig. 6. Partial-wave inelastic cross sections for I = 1/2 from Morgan (Ref. 7). The ordinate is all inelastic channels, therefore is only an upper limit for $\pi N \rightarrow \pi\pi N$.

Fig. 7a. Possible partial-wave decomposition in the production of three particles. For $\pi\pi N$, only one has spin, but for generality we assume the nucleon may be either particle 1, 2, or 3, so we distinguish between, e.g., ℓ_{12} and j_{12}.

Fig. 7b. The three amplitudes used in the isobar model.

Fig. 8. Summary of partial waves for I = 1/2, $\pi N \rightarrow \pi\pi N$, from various published analyses (Refs. 7, 10, 15, 17, 18, 21). The horizontal bars show the energy regions in which the partial waves listed on the left-hand side are present, according to the various analyses. Wiggly arrows symbolize the projections made by Namyslowski et al. (NRR), Ref. 18. For further explanations, see text.

Fig. 9. η production cross section (top), and Legendre polynomial expansion coefficients of the η differential cross section, from Ref. 25. The cross-section values are for only the 34% of η

which decay into $\gamma\gamma$. The η production cross section is compared with the S_{11} inelastic cross section predicted by various EPSA's.

Fig. 10. Coefficients in the Legendre polynomial expansion $d\sigma/d\Omega = \lambda\!\!\!^{-2} \Sigma A_\ell P_\ell (\cos\theta)$ of the differential cross section for the reaction $\pi^- p \to \Lambda K^0$. Note that θ is the c.m. angle between the momenta of π^- and Λ. No A_ℓ with $\ell > 4$ were required for adequate fits in this momentum region. The total cross section for this reaction is given by $\sigma(\pi^- p \to \Lambda K^0) = 4\pi \lambda\!\!\!^{-2} A_0$ (from Ref. 26).

Fig. 11. Argand plots for partial-wave amplitudes in the reaction $K^- p \to \pi\Sigma$, from Ref. 27.

Fig. 12. Plots of g_s versus g_a from Tripp et al. (Ref. 30). Error bars on the heavy and medium lines correspond respectively to 25% and 50% uncertainty in the decay rates. Light lines are uncertain to a factor $\geqslant 2$. Long-dashed lines denote upper limits. Short-dashed lines indicate the regions of the figures allowed by measurements of the relative signs of reaction amplitudes by Kernan and Smart and by the CERN-Heidelberg-Saclay collaboration. The sign affixed to each decay-rate line denotes the sign of the amplitude in Eq. (9). Shaded areas in each figure indicate the approximate values of g_s and g_a that seem to agree best with experiment, although other regions of each plot may still be acceptable. Wavy lines in Fig. 12(b) exhibit the displacements from the pure singlet and pure octet decay rates into $\Sigma\pi$ and $N\bar{K}$ due to a mixing angle of -16 deg, the magnitude suggested by the mass formula.

Fig. 13. Illustration of the sign determination of Y^* decay amplitudes. Signs indicated by (+) or (-) are those of the amplitude A in Eq. (9).

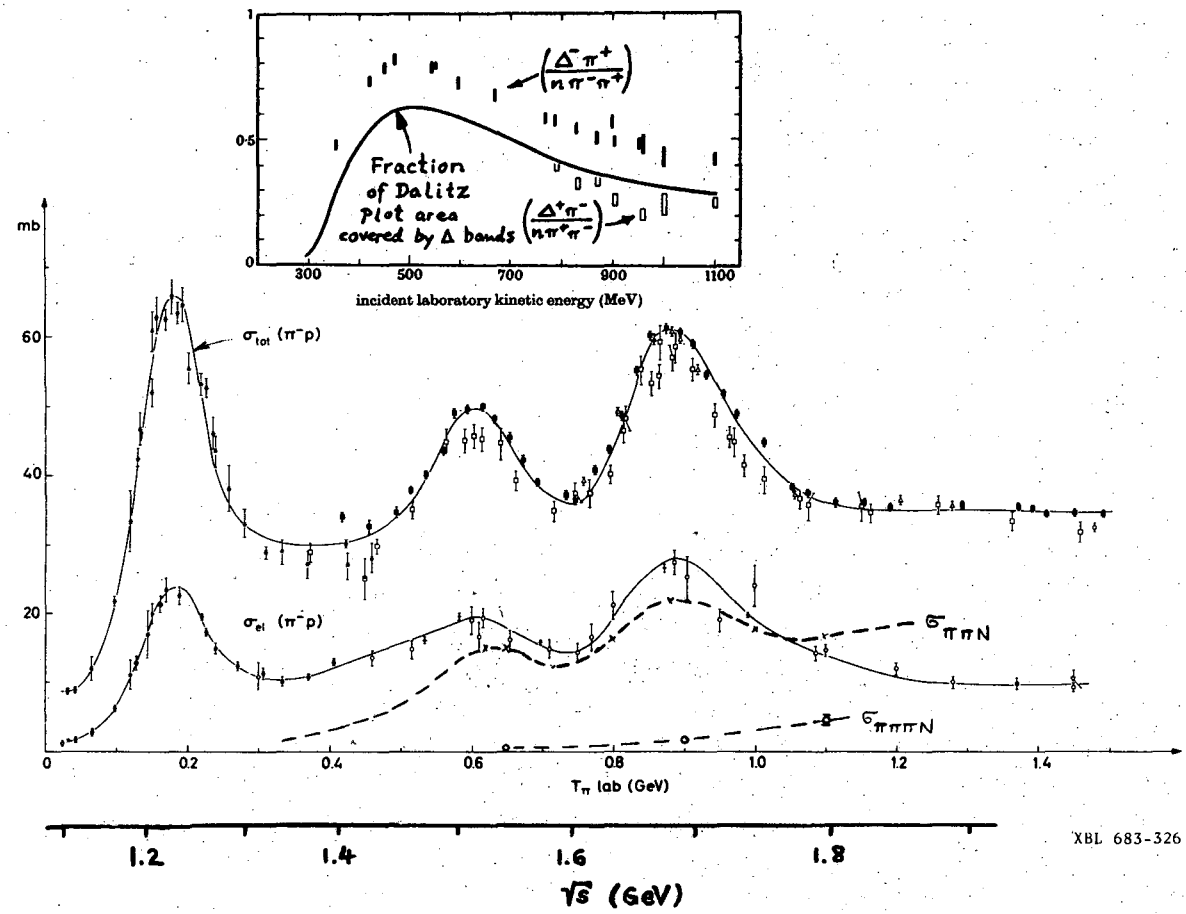
Fraction of Dalitz plot area covered by Δ bands
incident laboratory kinetic energy (MeV)
mb
σtot (π⁻p)
σel (π⁻p)
σππN
σπππN
Tπ lab (GeV)
√s (GeV)
XBL 683-326

Fig. 1

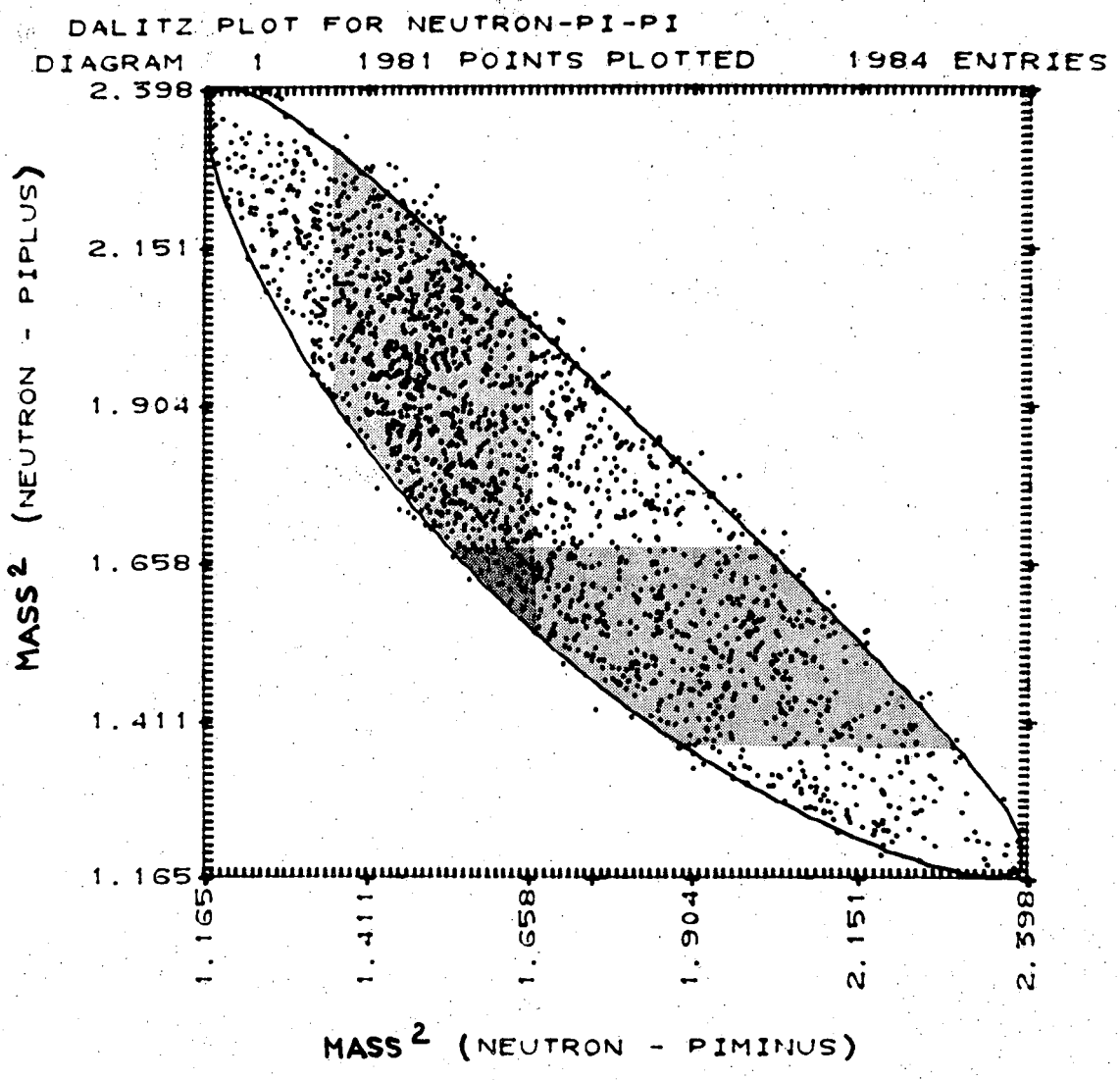

XBL 683-324

Fig. 2

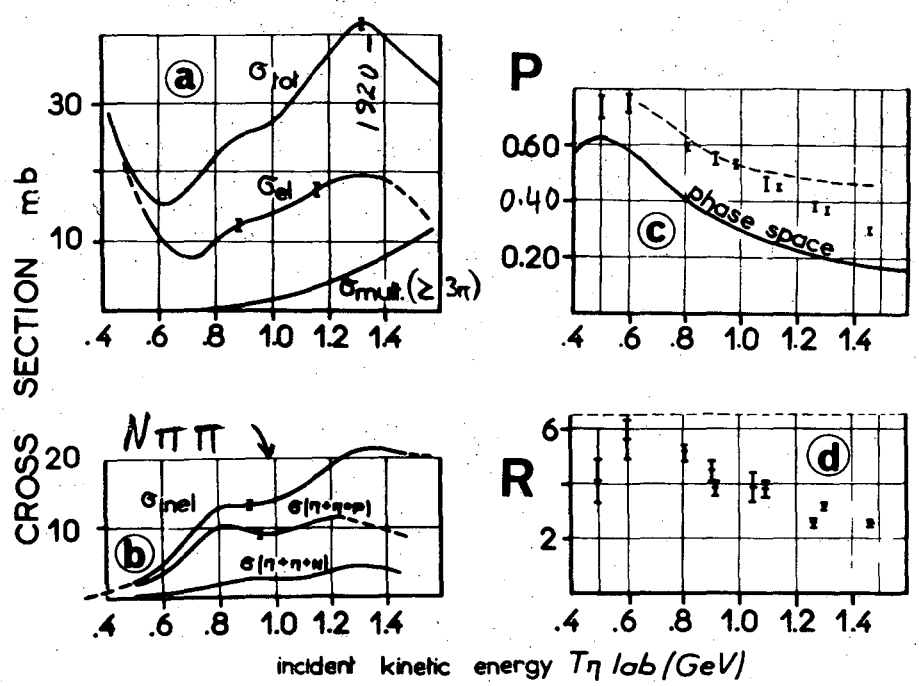

(a) Total (σ_{tot}), elastic (σ_{el}), and multipion-production (σ_{mult}) cross sections for π^+p interaction from 0.4 to 1.4 GeV. (b) Total inelastic (σ_{inel}) and single-pion-production ($\sigma_{\pi^+p\pi^0}$ and $\sigma_{\pi^+\pi^+n}$) cross sections. (c) Ratio P of the number of events in the isobar mass ($p\pi^+$) region (1.23 ± 0.07 GeV/c^2) to the total number of $\pi^+p\pi^0$ events compared with phase space (continuous line) and isobar-model (dashed line) predictions. (d) Ratio R of the cross section $\sigma_{\pi^+p\pi^0}$ to the cross section $\sigma_{\pi^+\pi^+n}$, and the isobar-model prediction (dashed line).

XBL 682-175

Fig. 3

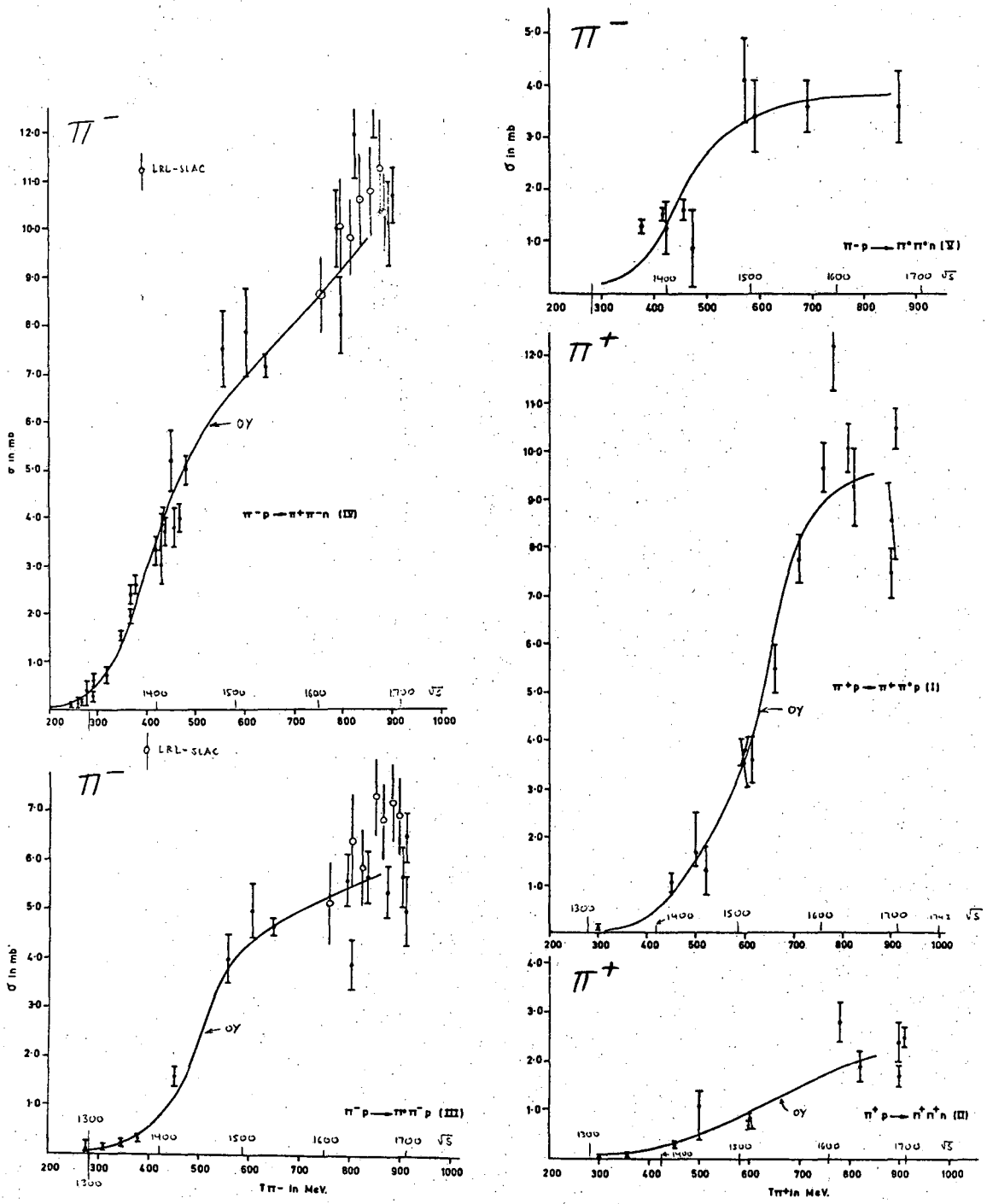

XBL 682-176

Fig. 4

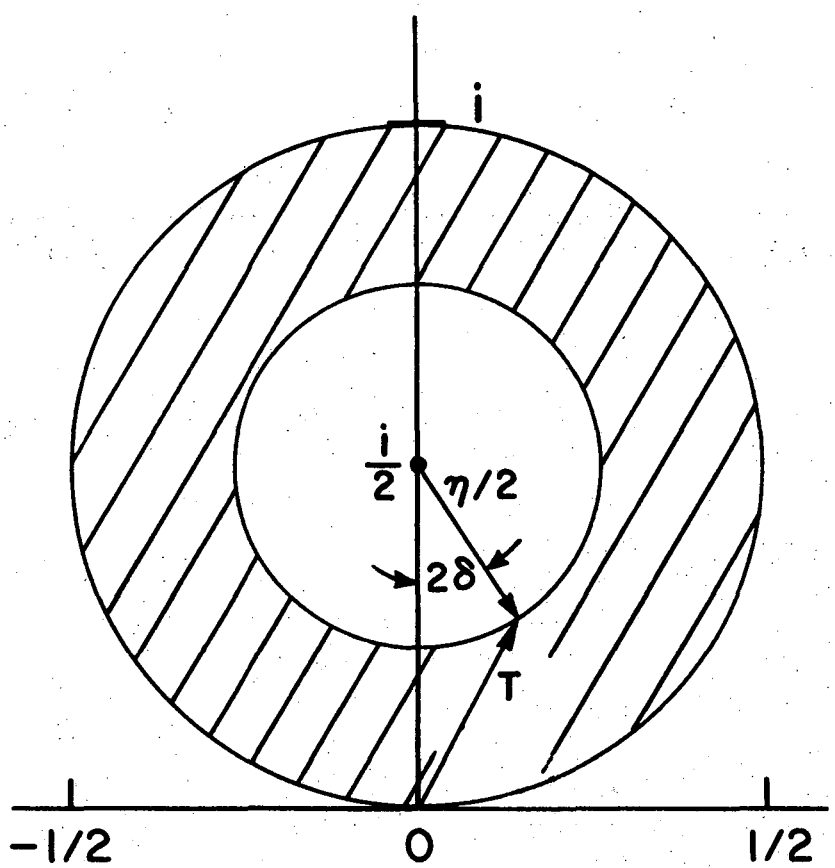

$$T = \frac{\eta e^{2i\delta} - 1}{2i}$$

XBL683-2117

Fig. 5

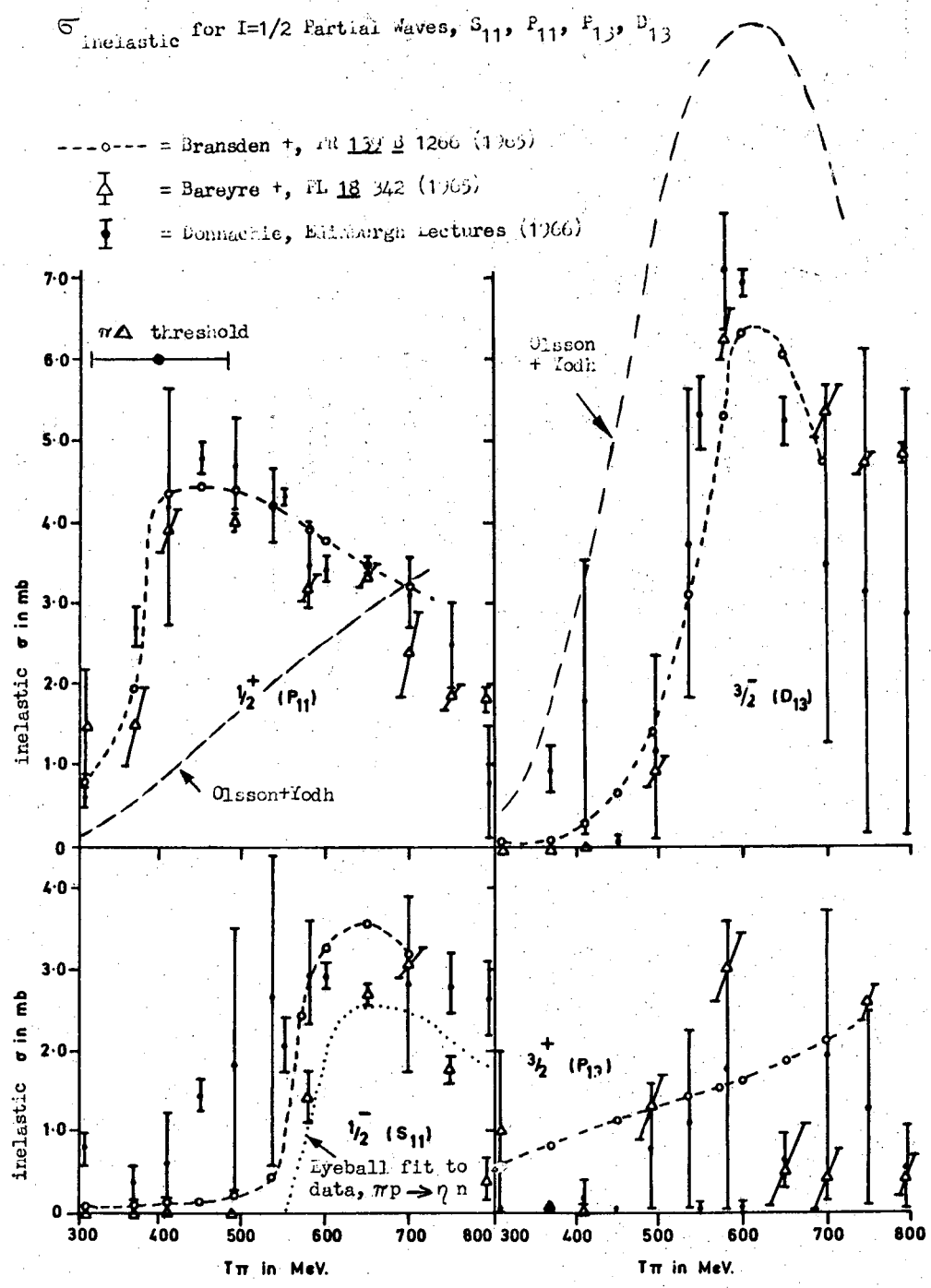
σ inelastic for I=1/2 Partial Waves, S11, P11, P13, D13
---o--- = Bransden +, PR 132 B 1266 (1963)
= Bareyre +, PL 18 342 (1965)
= Donnachie, Edinburgh Lectures (1966)
πΔ threshold
Olsson + Yodh
1/2+ (P11)
Olsson+Yodh
3/2− (D13)
1/2− (S11)
Eyeball fit to data, πp → η n
3/2+ (P13)
inelastic σ in mb
Tπ in MeV.
XBL 682-173

Fig. 6

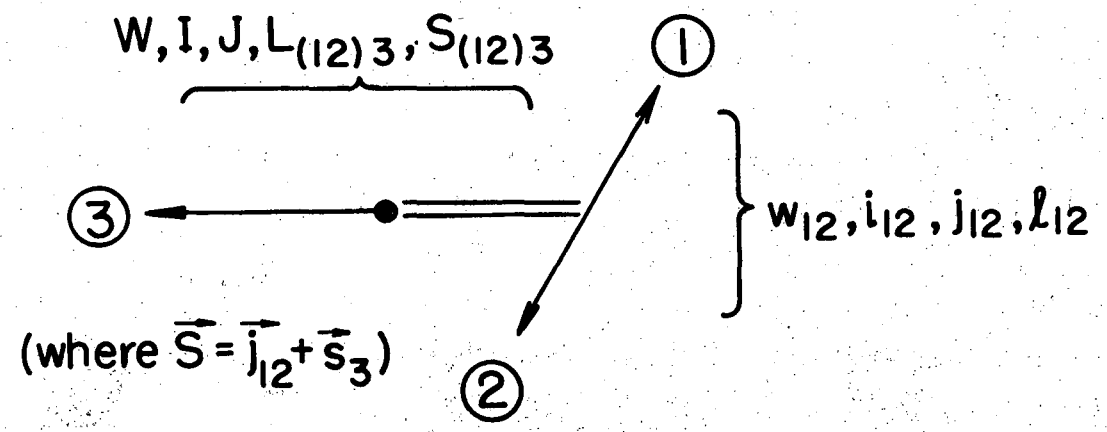

Fig. 7a

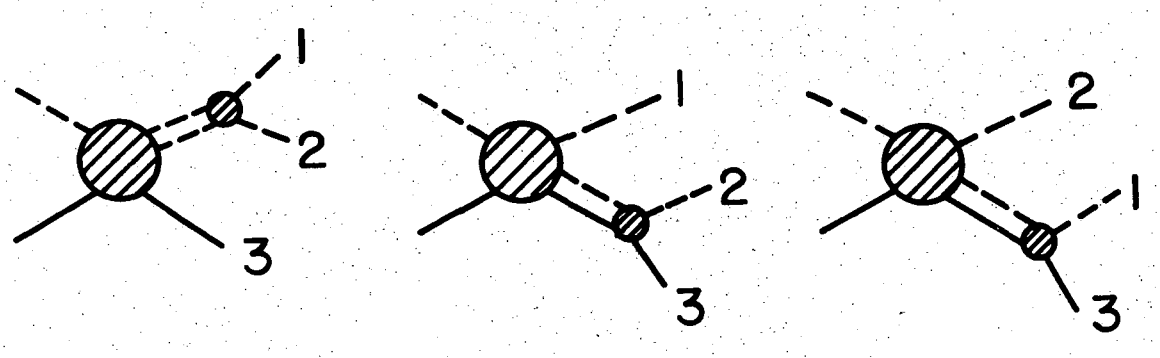

Fig. 7b

XBL682-1986

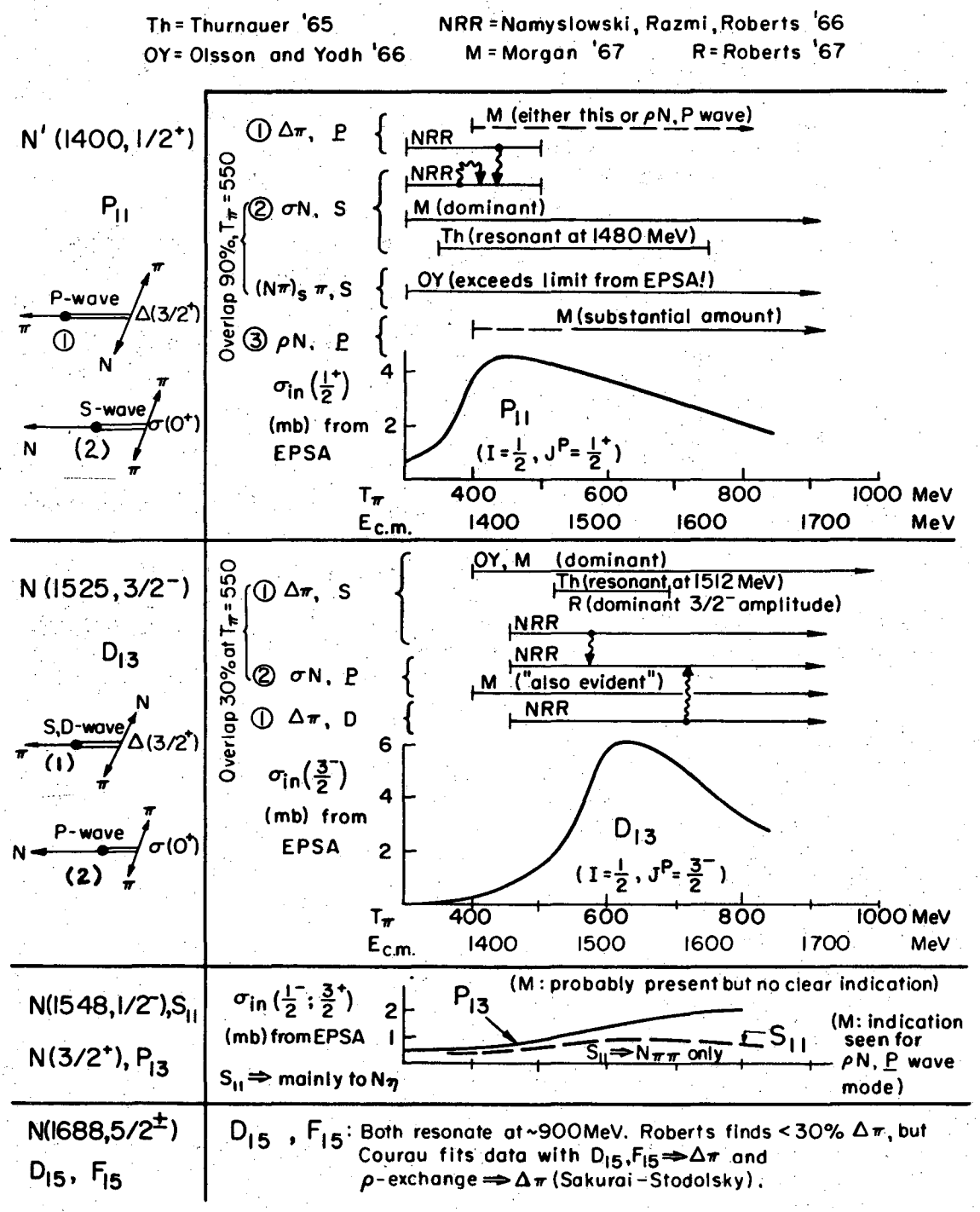
Th = Thurnauer '65
OY = Olsson and Yodh '66
NRR = Namyslowski, Razmi, Roberts '66
M = Morgan '67
R = Roberts '67
N' (1400, 1/2+)
P11
P-wave
Δ(3/2+)
S-wave
σ(0+)
Overlap 90%, Tπ = 550
① Δπ, P
② σN, S
(Nπ)s π, S
③ ρN, P
M (either this or ρN, P wave)
NRR
M (dominant)
Th (resonant at 1480 MeV)
OY (exceeds limit from EPSA!)
M (substantial amount)
σin (1/2+) (mb) from EPSA
P11
(I = 1/2, JP = 1/2+)
Tπ
Ec.m.
400 600 800 1000 MeV
1400 1500 1600 1700 MeV
N (1525, 3/2−)
D13
S,D-wave
P-wave
Overlap 30% at Tπ = 550
① Δπ, S
② σN, P
① Δπ, D
OY, M (dominant)
Th (resonant at 1512 MeV)
R (dominant 3/2− amplitude)
M ("also evident")
σin (3/2−) (mb) from EPSA
D13
(I = 1/2, JP = 3/2−)
N(1548, 1/2−), S11
N(3/2+), P13
σin (1/2−; 3/2+) (mb) from EPSA
S11 ⇒ mainly to Nη
P13
S11
S11 ⇒ Nππ only
(M: probably present but no clear indication)
(M: indication seen for ρN, P wave mode)
N(1688, 5/2±)
D15, F15
D15, F15: Both resonate at ~900 MeV. Roberts finds < 30% Δπ, but Courau fits data with D15, F15 ⇒ Δπ and ρ-exchange ⇒ Δπ (Sakurai-Stodolsky).
XBL682-1987

Fig. 8

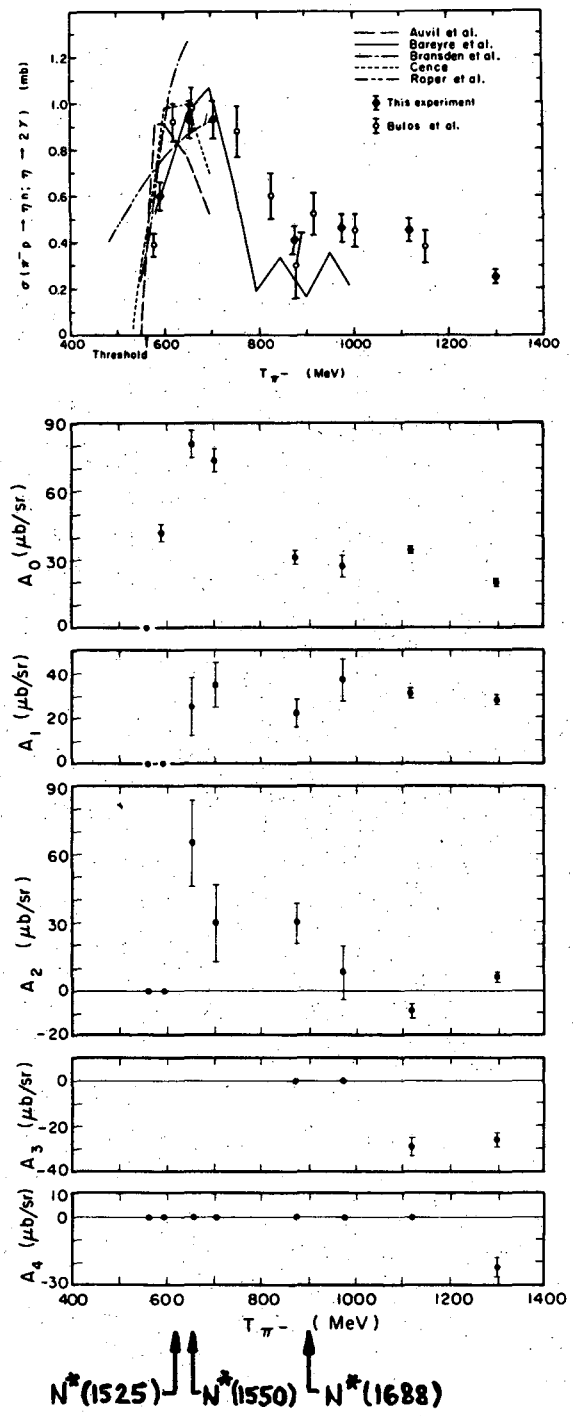

XBL 683-325

Fig. 9

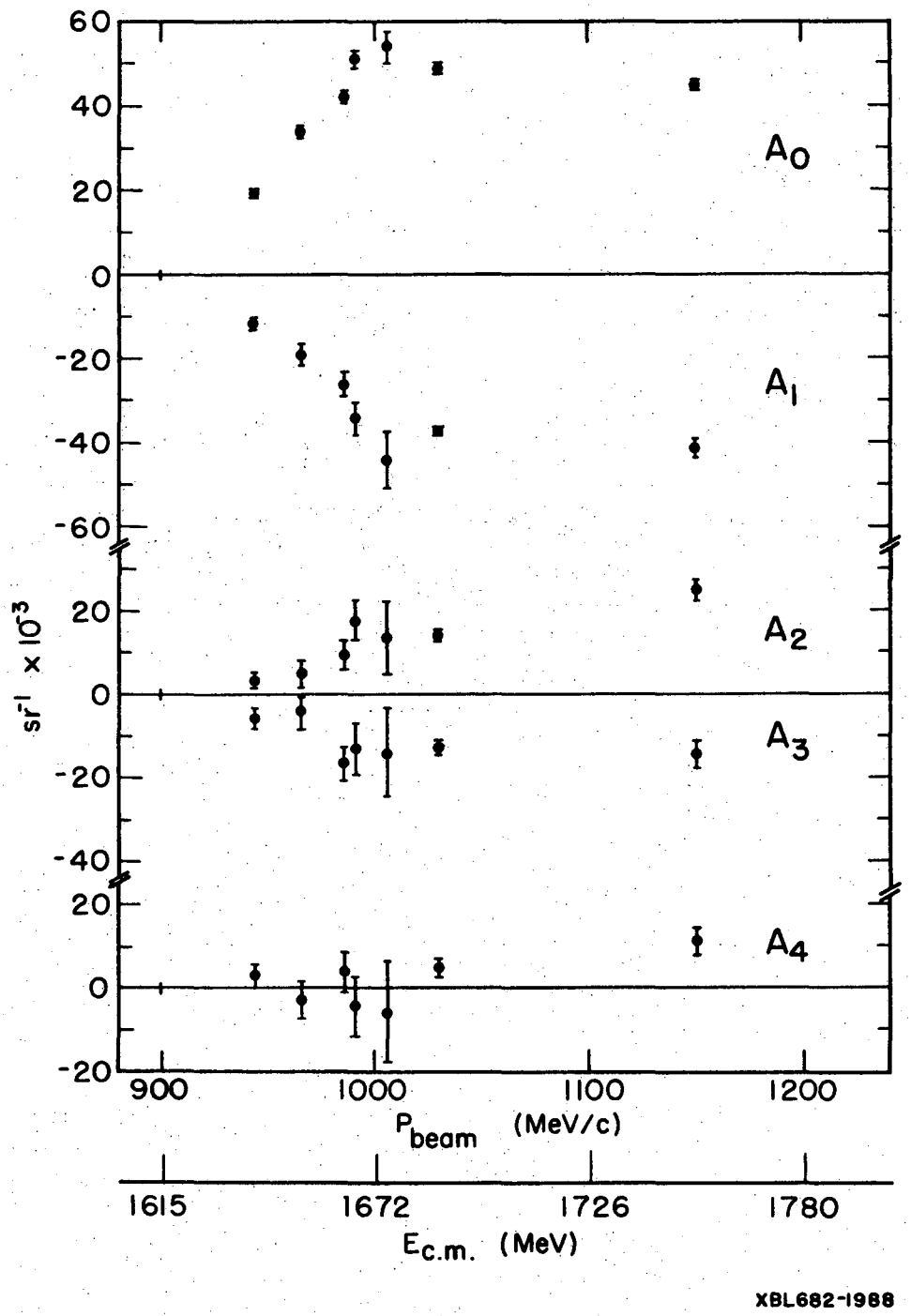
60
40
20
0
-20
-40
-60
20
0
-20
-40
20
0
-20
A_0
A_1
A_2
A_3
A_4
$sr^{-1} \times 10^{-3}$
900
1000
1100
1200
P_{beam} (MeV/c)
1615
1672
1726
1780
$E_{c.m.}$ (MeV)
XBL682-1988

Fig. 10

Argand Plots from C.H.S. $K^- p \Rightarrow Y^* \Rightarrow \pi \Sigma$

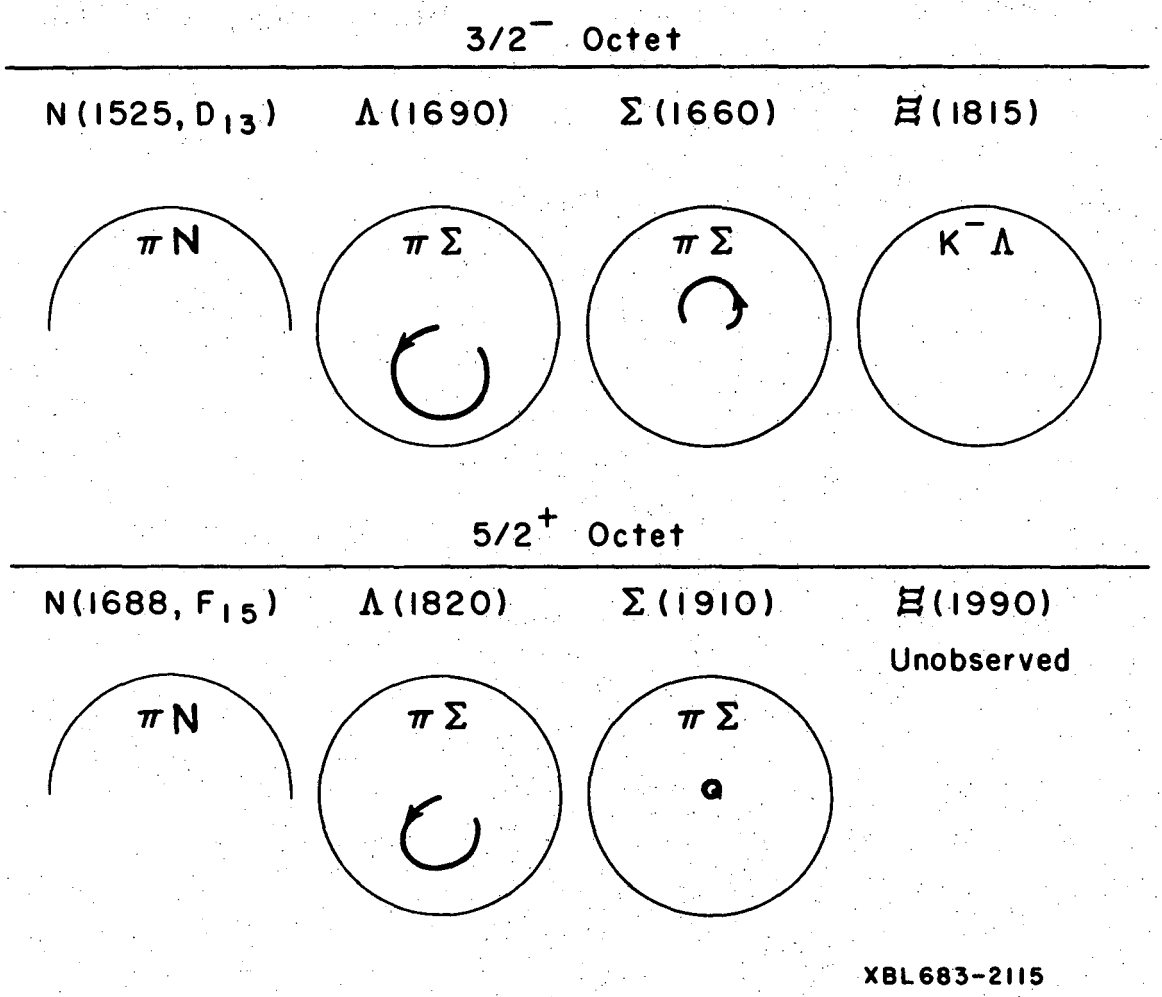

Fig. 11

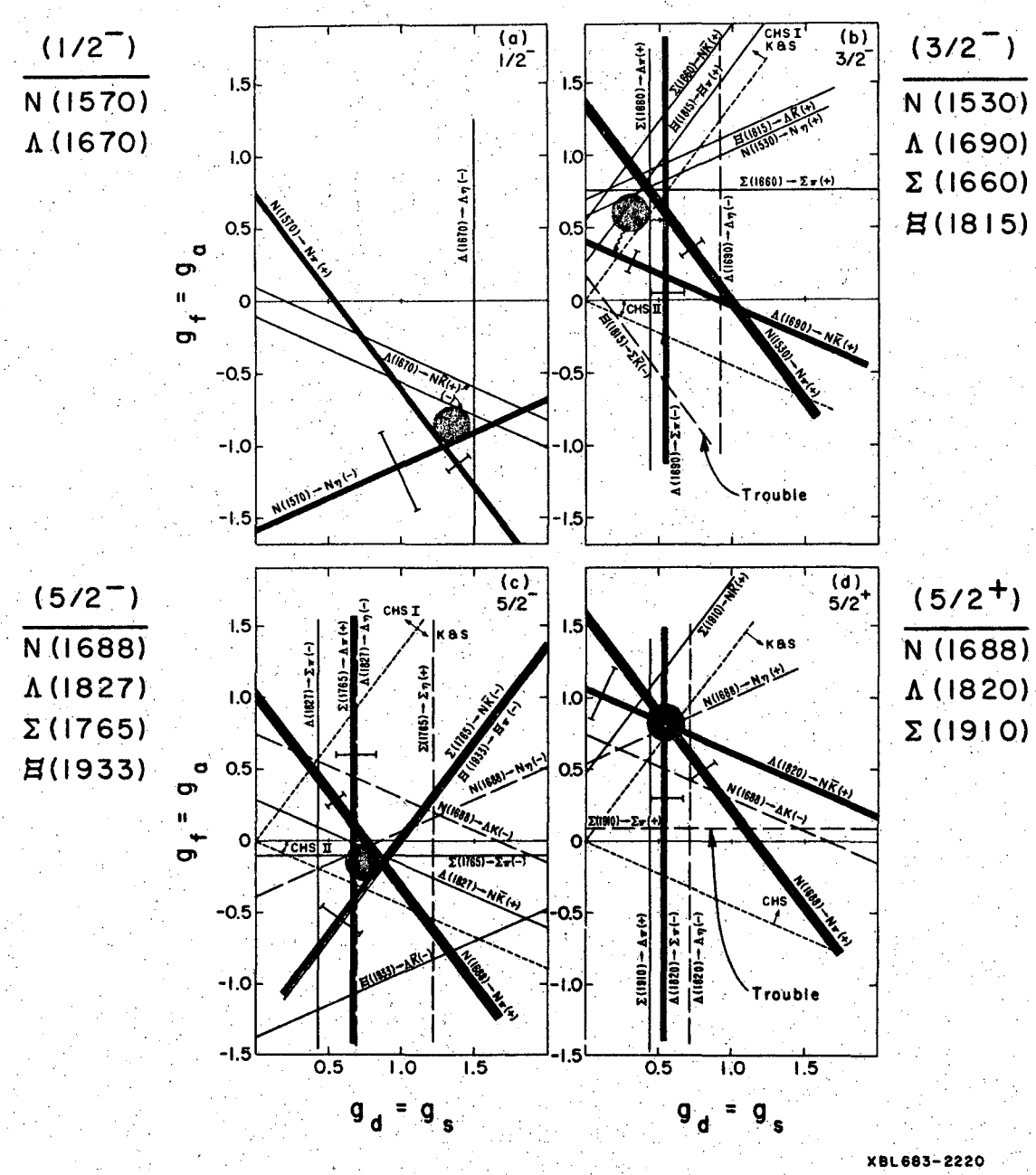
(1/2⁻)
N (1570)
Λ (1670)
(3/2⁻)
N (1530)
Λ (1690)
Σ (1660)
Ξ (1815)
(5/2⁻)
N (1688)
Λ (1827)
Σ (1765)
Ξ (1933)
(5/2⁺)
N (1688)
Λ (1820)
Σ (1910)
(a) 1/2⁻
(b) 3/2⁻
(c) 5/2⁻
(d) 5/2⁺
CHS I
Kas
CHS II
CHS
Trouble
$g_f = g_a$
$g_d = g_s$
XBL683-2220

Fig. 12

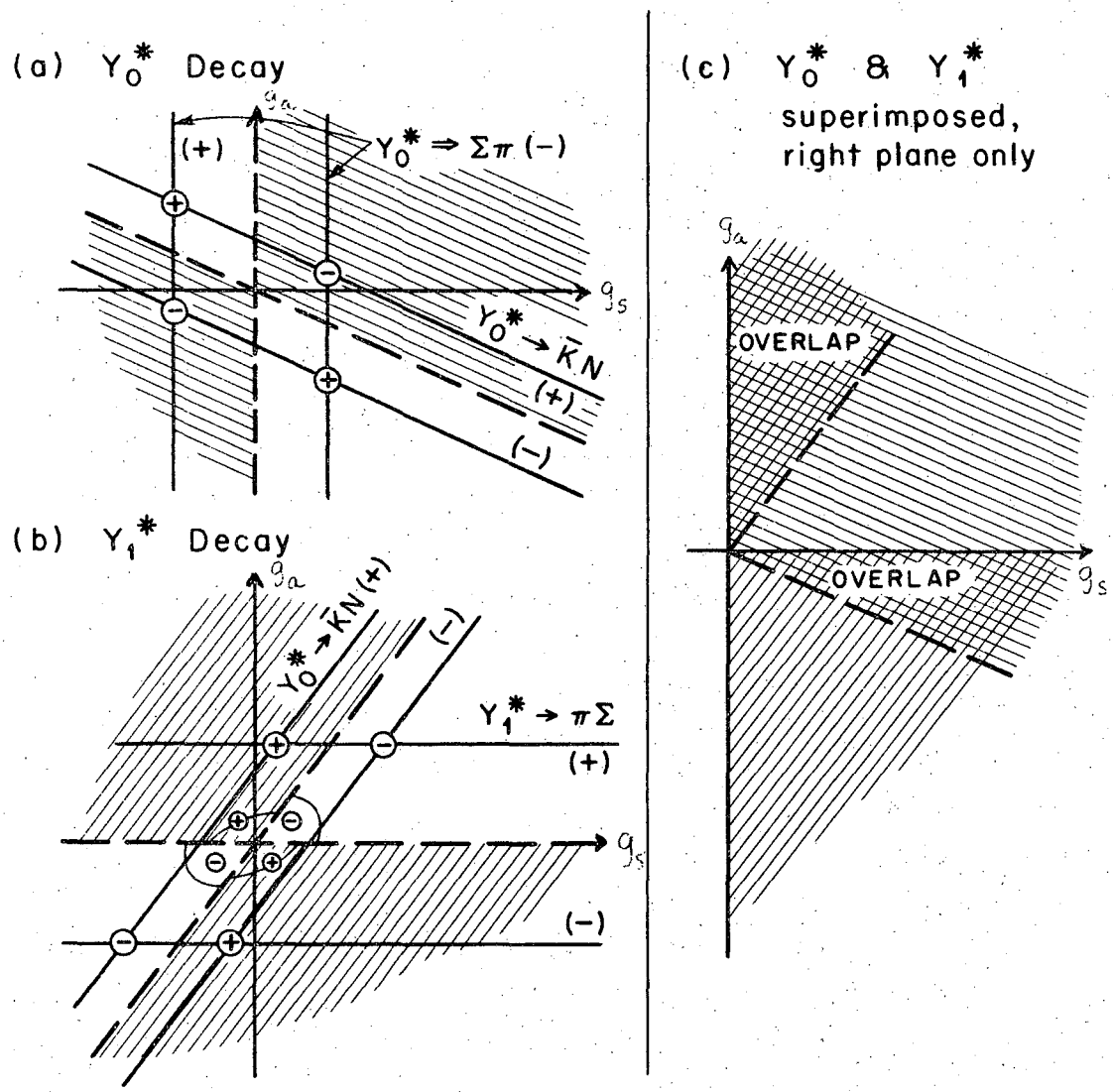

XBL683-2116

Fig. 13

This report was prepared as an account of Government sponsored work. Neither the United States, nor the Commission, nor any person acting on behalf of the Commission:

A. Makes any warranty or representation, expressed or implied, with respect to the accuracy, completeness, or usefulness of the information contained in this report, or that the use of any information, apparatus, method, or process disclosed in this report may not infringe privately owned rights; or

B. Assumes any liabilities with respect to the use of, or for damages resulting from the use of any information, apparatus, method, or process disclosed in this report.

As used in the above, "person acting on behalf of the Commission" includes any employee or contractor of the Commission, or employee of such contractor, to the extent that such employee or contractor of the Commission, or employee of such contractor prepares, disseminates, or provides access to, any information pursuant to his employment or contract with the Commission, or his employment with such contractor.